

AMERICAN UNIVERSITY OF BEIRUT

EFFECTIVENESS OF UPPER-ROOM UVGI IN SPACES
CONDITIONED BY LOCALIZED AIR-CONDITIONING
SYSTEMS: ENHANCING AIR QUALITY AND ENERGY
PERFORMANCE

by
MOHAMAD ISSAM KANAAN

A dissertation
submitted in partial fulfillment of the requirements
for the degree of Doctor of Philosophy
to the Department of Mechanical Engineering
of the Faculty of Engineering and Architecture
at the American University of Beirut

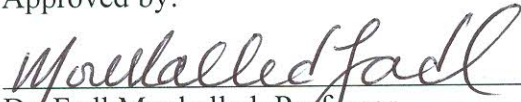
Beirut, Lebanon
February 2015

AMERICAN UNIVERSITY OF BEIRUT

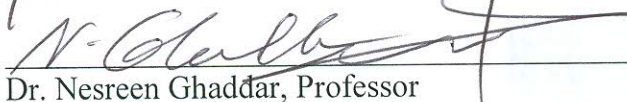
EFFECTIVENESS OF UPPER-ROOM UVGI IN SPACES
CONDITIONED BY LOCALIZED AIR-CONDITIONING SYSTEMS:
ENHANCING AIR QUALITY AND ENERGY PERFORMANCE

by
MOHAMAD ISSAM KANAAN


Approved by:



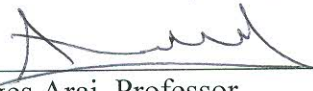
Dr. Fadl Moukalled, Professor
Department of Mechanical Engineering, AUB
Chairperson of Committee



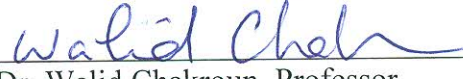
Dr. Nesreen Ghaddar, Professor
Department of Mechanical Engineering, AUB
Advisor



Dr. Kamel Ghali, Professor
Department of Mechanical Engineering, AUB
Co-advisor



Dr. Georges Araj, Professor
Department of Pathology and Laboratory Medicine, AUB
Member of Committee



Dr. Walid Chakroun, Professor
Department of Mechanical Engineering, Kuwait University
Member of Committee



Dr. Mohamad Hosni, Professor
Department of Mechanical Engineering, Kansas State University
Member of Committee

Date of dissertation defense: February 6, 2015

AMERICAN UNIVERSITY OF BEIRUT

DISSERTATION RELEASE FORM

Student Name: Kanaan Mohamad Issam
Last First Middle

Master's Thesis Master's Project Doctoral Dissertation

I authorize the American University of Beirut to: (a) reproduce hard or electronic copies of my thesis, dissertation, or project; (b) include such copies in the archives and digital repositories of the University; and (c) make freely available such copies to third parties for research or educational purposes.

I authorize the American University of Beirut, **three years after the date of submitting my dissertation** to: (a) reproduce hard or electronic copies of it; (b) include such copies in the archives and digital repositories of the University; and (c) make freely available such copies to third parties for research or educational purposes.



Signature

Feb 17, 2015

Date

ACKNOWLEDGMENTS

I would like to express my special appreciation and thanks to my advisor Prof. Nesreen Ghaddar and co-adviser Prof. Kamel Ghali. You have been tremendous mentors for me. I would like to thank you for encouraging my research and providing me with needed support. I would also like to thank Prof. Georges Araj for his valuable contribution in the bacterial part of my work and for serving as a member of my dissertation committee. Special thanks to Prof. Fadl Moukalled, the chair of my committee, and Prof. Walid Chakroun and Prof. Mohamad Hosni for serving as my committee members even at hardship. I also want to thank you for your brilliant comments and suggestions.

I would also like to thank all of my friends and colleagues who often supported me and incited me to strive towards my goal: Amer Keblawi, Mohammad Habbal, Mohammad Allouche, Mohammad Baassiri, Hussein Maanieh, Khaled Abou Hweij, Mohammad Rida, Nagham Ismail, Hanin Hamdan, Hajar Fawaz, Raghid Farhat, and Carine Habchi. Your presence has always been a source of joy and motivation, and your compassion is highly appreciated.

Very special thanks to my colleague and close friend Abed AlKader Al Saidi. You have always been my support in the moments when there was no one to answer my queries. It will never be forgotten that I found my first position because of you.

I would also like to thank my special friend Ahmad Nsouly for his continuous care and encouragement.

Special thanks to my family. Words cannot express how grateful I am to my mother for all the sacrifices that she has made on my behalf. Your prayer for me was what sustained me thus far. The encouragement of my siblings is also highly valued.

At the end, I would like to express appreciation to my beloved fiancée Hiba who has always been my support in the hard times. Your true love and faithfulness are highly appreciated.

AN ABSTRACT OF THE THESIS OF

Mohamad Issam Kanaan for Doctor of Philosophy
Major: Mechanical Engineering

Title: Effectiveness of Upper-room UVGI Systems in Spaces Conditioned by Localized Air Conditioning Systems: Enhancing Air Quality and Energy Performance

Providing thermal comfort and good indoor air quality (IAQ) at minimal energy cost has been considered a priority in the field of heating, ventilation, and air conditioning (HVAC) for the past couple of decades. It is widely known that the use of return air in any air-conditioning system results in a decrease in its energy consumption, but also results in high pollutant and bacteria concentrations that may reach unacceptable levels in the occupied zone. One of the plausible methods used for air disinfection is the Upper-Room Ultraviolet Irradiation (UR-UVGI) systems that can effectively inactivate airborne bacteria, especially if there is air mixing between the upper irradiated zone and lower occupied zone.

This work aims to investigate by modeling and experimentation the effectiveness of UR-UVGI in improving air quality in localized air conditioning systems: 1) vertical localizing mixed Displacement Ventilation (DV) combined with Chilled Ceiling (CC) system; 2) horizontal localizing (zoning) using ceiling diffuser that emits the air from the perimeter (sides) while the air return is through the center ensuring that the returned air from the conditioned zone is taken upward to be reused.

A commercial computational fluid dynamics (CFD) software is used to simulate the flow, thermal, and species transport in the conditioned space. The airborne bacteria transport and its decay when UV field is present are simulated using Eulerian approach and neglecting gravitational effects; whereas the gravitational settling and deposition effects of large bacteria-carrying particles are simulated using Lagrangian method. The air flow and thermal boundary conditions of the diffuser are obtained from experiments and are used as inputs to the CFD models. The CFD models are validated using air velocity and temperature measurements made at several positions in two climatic chambers to test both horizontal and vertical localization/zoning systems.

Since the vertical localization system (CC/DV) is based on vertical transport, a simplified multilayer model is developed and experimentally validated to predict the bacteria dispersion and deposition at different droplet sizes in mixed CC/DV rooms

with and without UR-UVGI. The results of the simplified model are compared with CFD predictions of bacteria transport and deposition. The validated simplified model can be also used to determine the maximal allowable mixing ratio for acceptable IAQ with and without the use of UR-UVGI.

In addition, the prospective energy savings obtained from using the return air and UR-UVGI in both HVAC systems considered in this thesis are evaluated.

CONTENTS

ACKNOWLEDGEMENTS.....	v
ABSTRACT.....	vi
LIST OF ILLUSTRATIONS.....	x
LIST OF TABLES.....	xii
Chapter	
I. INTRODUCTION.....	1
II. THE STATE OF ART OF UVGI.....	7
A.Indoor Bioaerosol Sources	7
1. Human Expiratory Activities	8
2. Biologically Contaminated HVAC Systems	10
B.UVGI Systems	11
1. Air Disinfection Systems	11
2. Upper Room UV Safety	13
3. UV Lamp Modeling	13
4. Measuring UV Irradiation	15
5. UVGI Efficacy Evaluation	16
6. Factors on UR-UVGI Performance.....	16
C.Upper Room UVGI with Localized Air-Conditioning Systems	18
1. Horizontal Localizing Air Distribution System	18
2. Vertical Localizing Air Distribution (CC/DV) System.....	19
III. OBJECTIVES AND SCOPE.....	22
A.Objectives	22
B. Scope.....	22

IV. RESEARCH METHODOLOGY	24
V. CFD METHODS	30
A. Flow and Thermal transport	31
B. Bacteria Transport and UV Inactivation.....	33
1. Eulerian Model	34
2. Lagrangian Tracking Model.....	37
VI. EXPERIMENTAL METHODS	39
A. Room with Horizontal Air Localization System.....	39
B. Room with Vertical Air Localization (CC/DV) System	41
C. Air Flow Measurements	42
D. Thermal Measurements	43
E. UV Field Measurements	44
F. Measurements of airborne bacteria concentration and bacteria settling	45
VII. SIMPLIFIED MODELING OF PATHOGEN TRANSPORT UVGI SPACES CONDITIONED WITH CC/DV	48
A. Plume Multi-zone Multi-layer Model for Airborne Transport of Pathogens.....	48
B. Extended Plume Multi-zone Multi-layer Model for Pathogen Transport at Different Particle Sizes	57
VIII. RESULTS AND DISCUSSION	60
A. Horizontal Air Localization System.....	60
1. Experimental Validation of the CFD Model	60
2. Validation of the CFD-UV Model with Published Data	65

B. Vertical Air Localization (CC/DV) System	66
1. Experimental Validation of the CFD Model	66
2. CFD Validation of the Airborne Bacteria Transport Plume Multi-layer Multi-zone Model (with no deposition)	67
3. Experimental Validation of the extended simplified model (for small droplets)	72
4. Experimental Validation of the CFD Model for Bacteria Deposition (for small droplets).....	74
5. CFD Substantiation of the Simplified Model (for large droplets)	76
6. Effect of the Droplet Size.....	77
IX. CASE STUDIES	80
A. Case Study 1 (horizontal air localization system).....	80
1. Results without the Use of UVGI	82
2. Results with the Use of UVGI.....	83
3. Energy Analysis	84
B. Case Study 2 (vertical air localization CC/DV system)	85
1. Results without the Use of UVGI:	86
2. Results with the Use of UVGI:	87
3. Energy Analysis	87
X. CONCLUSIONS AND FUTURE WORK.....	90
BIBLIOGRAPHY	96

ILLUSTRATIONS

Figure	Page
1. Illustrations of (a) horizontal localization (zonal) airflow and (b) vertical localization in CC/DV system.	25
2. Flow chart of the inputs and predicted outputs of the various models.	27
3. Grids generated by ANSYS mesher for the (a) horizontal localizing air flow room (1,500,000 elements) and vertical air localization (CC/DV) room for (b) Eulerian simulations (1,270,000 elements) and (c) Lagrangian simulations (1,700,000 elements).....	32
4. Schematics of the climatic room (a) side view, (b) top view, and (c) top view showing the positions of actinometrical measurements	40
5. Schematics of the CC/DV room (a) isometric view showing the vertical sampling plane (V) and horizontal planes (B, S, and E), and (b) top view showing the locations of the air sampling hoses. H_s denotes the stratification height.	42
6. Pictures showing the (a) heated cylinders, air sampling hoses, atomizer, and (b) air sampling hoses connected to impingers	47
7. Schematic of the zonal distribution of DV room equipped with UVGI.	50
8. Schematic of mathematical model with upper UV field.....	54
9. Plot of the measurements and CFD predictions of air velocity at 8 labeled positions on the jet profile diagram.	61
10. Plot of the predicted and measured temperatures in the vicinity of (A) cylinder 3 and (B) cylinder 4.	62
11. Plots of (A) the velocity distribution in the room, (B) air temperature distribution, (C) <i>S. marcescens</i> distribution when UVGI is OFF and (D) <i>S. marcescens</i> distribution when the three un-louvered 18 W UV lamps are operated.....	63
12. Plot of bacteria concentration of in the large space with two ceiling localized system when bacteria is emitted in one zone.	64

13. Comparative plot of measured and CFD values of room air temperature distribution.....	67
14. Room velocity vector field.	68
15. (a) Thermal field and (b) CO ₂ mass fraction distribution in the room.	69
16. Contour plots of bacteria mass fraction when UV lamps are OFF on horizontal cut planes at (a) $z = 1.28$ m, (b) $z = 2$ m, and on the sampling plane when UV lamps are (c) ON and (d) OFF.	70
17. Plots of the results using the multi-layer model and the CFD simulation predictions of bacteria concentrations as a function of height for room air (a) without use of UV and (b) with use of UV.....	71
18. Comparative plot of measurements and model predictions for <i>S. marcescens</i> concentrations for (a) $m_s = 0.11$ kg/s and (b) $m_s = 0.22$ kg/s	73
19. Petri plates after incubation for one pair of experiments.....	74
20. Comparison between experimental data and numerical bacteria deposition with and without the use of UVGI for (a) $m_s = 0.11$ kg/s and (b) $m_s = 0.22$ kg/s	75
21. <i>S. marcescens</i> concentration contour plots on the sampling plane for $m_s = 0.11$ kg/s (a) when UVGI is OFF and (b) when UVGI is ON.....	76
22. Plots of bacteria concentration using the multi-layer model and the CFD simulation predictions as a function of height for room air (a) without the use of UVGI and (b) with the use of UVGI.	77
23. Variations of bacteria concentration with height for droplet sizes 2.5, 10, 15, and 20 μm with and without the use of UVGI.....	78
24. Schematics of the office space (A) side view and (B) top view.	80
25. Variations of C/C_{max} for both CO ₂ and <i>S. marcescens</i> with their respective return air mixing ratios.	82
26. <i>S. marcescens</i> distribution for (A) 100% fresh air, (B) 11% return mixing ratio, and (c) 23% return mixing ratio.....	83
27. Contour plots of <i>S. marcescens</i> concentration field for $x = 0.23$ when 15 W UV is delivered to the space.	84
28. Comparison of the horizontal air localization system electrical consumption during the peak hour on a typical day of June, July, and August for different mixing ratios.	85

29. Variation of critical mixing ratios with stratification height based CO₂ concentration and bacteria concentration standard limits in the occupied zone. 87
30. Comparison of the system electrical consumption for different mixing ratios and UVGI setups 89

TABLES

Table	Page
1. Boundary conditions of the simulations.	37
2. Experimental scenarios	45
3. Distribution of UV irradiance in W/m^2 inside the horizontal air localization room.....	62
4. Velocity measurements and values obtained from CFD	66

CHAPTER I

INTRODUCTION

The building sector is a major contributor to energy consumption worldwide and its contribution is expected to increase in the upcoming years. In fact, the building sector accounted for 41.1% of the total energy consumption in the United States in 2011 and this figure is expected to increase to 42.1% in 2035 (U.S. Department of Energy, 2012). Furthermore, the *HVAC* system acquires the prime share of the energy consumption and can account in some cases for 70% of the total energy consumption of buildings (Chakroun et al, 2011). While researchers have used different strategies and hybrid systems to reduce the *HVAC* energy consumption, the common approach of these strategies is to increase the portion of return air in the supplied air and to use the air conditioning and fresh air only when it is needed. However, the well being of the occupants precludes energy conservation strategies that would otherwise prove effective. In many cases, increasing the amount of return air would increase the permissible CO₂ fraction and the circulated infectious particles jeopardizing the role of the air conditioning system in providing healthy environment to occupants. Therefore, targeting energy cost associated with providing good *IAQ* in *HVAC* systems is a strategic intervention to reduce building energy consumption (Sozer et al. 2011).

The *HVAC* industry is moving more towards localizing the air conditioning needs of occupants in buildings to minimize energy cost. To this end, the displacement ventilation (*DV*) has gained popularity because of its effectiveness and superiority in maintaining clean and contaminant free air in the occupied lower zone (Keblawi et al.,

2009, Ghaddar et al., 2008, Mossolly et al., 2008, Jiang and Reddy, 2007). In this system the pollutants are moved upward to the upper recirculated zone, which extends the localization over the entire space area, which means that the air zoning is vertical. Other systems such as localized air conditioning systems can achieve horizontal air zoning by dividing the space into separate zones without partition walls. Localized airflow results in both temperature and pollutant concentration segregations with limited air mixing between zones which provide more control on transmission of indoor contaminants (Lo and Novoselac, 2010).

Researchers have considered possible modifications on those systems to enhance their performance and reduce energy consumption. For example, in displacement ventilation, the stratification height was lowered to about 1.2 m for seated occupants and return air was mixed with fresh air in the supply air. In localized air conditioning systems, the peripheral angled supply air with a central return air diffuser is used to reduce mixing with the space air resulting in a larger portion of the return zone air in the supply air. Containing the localized zone and increasing the portion of return air in the air supplied to the zone are effective in minimizing energy cost in both systems but at the expense of increasing the contaminant concentrations and spread of bioaerosols within the localized zone.

Airborne infection has always been a major source of morbidity and mortality worldwide (Corbett et al. 2003).

Cold and influenza are two of the most common - not the most severe - airborne infectious diseases. Several of those diseases are related to huge death tolls in the far and near past such as Severe Acute Respiratory Syndrome (SARS) and Tuberculosis (TB). Viboud et al. (2004) reported a total of 1.87 million deaths caused by TB

infections in about 22 countries. Moreover, there were 8098 people infected by SARS, 774 of whom died according to WHO statistics (2004). Hence, microbiological air quality is an important criterion for safe working environment.

The World Health Organization (WHO, 1988) recommended not more than 50 colony forming units (*CFU*) of fungi/m³ and a maximum number of bacteria of 100 *CFU* /m³ of air for hospital environments. In office spaces, the maximum allowable limit of bacterial and fungal count is 500 *CFU*/m³ although some researchers suggested that the counting of human normal flora bacteria above 200 *CFU*/m³ in the air would be considered high (Ismail et al., 2010; Ross et al., 2004; Morey et al., 1986).

The constraint of indoor bacteria concentration would pose prohibitive ventilation requirement contributing to increased cooling load and energy consumption. This has led to consideration of other methods that can disinfect air such as ultraviolet germicidal irradiation (*UVGI*). This method uses the *UV* light at sufficiently short wavelength to inactivate microorganisms. The indoor air bacterial concentration may then be reduced by inactivating bacteria at minimal energy cost, instead of diluting the air by supplying significant amounts of fresh air.

For *UR-UVGI* to be effective, the infectious particles generated by a person should be moved from the lower occupied part of the room to the upper part where the lamps are located. In many literature articles, researchers rely on turbulence for achieving the transport of germs from the lower occupied part of the space to the upper irradiated zone (Riley and Kaufman, 1972; Noakes et al., 2004; Beggs and Sleight, 2002).

Zhu et al. (2013) found out using *CFD* that air exchange rate is the decisive factor in evaluating the effectiveness of *UR-UVGI* in disinfecting indoor air and that the

use of a ceiling fan would improve the germicidal performance in general. Miller and Macher (2000) developed and tested the steady-state and decay experimental methods to quantify the efficacy of *UR-UVGI* in inactivating airborne bacteria. They reported that the performance of *UR-UVGI* depends on many factors of which the most important is the type of targeted bacteria.

Modeling approaches to study upper-room *UVGI* either used *CFD* (Heidarinejad and Srebric, 2013; Zhu et al., 2012; Hathway et al., 2011; Beggs and Sleigh, 2002) or simplified two or three zone-mixing models (Sung and Kato, 2010; Nicas and Miller, 2009; Noakes et al., 2004). The *CFD* modeling provides relatively an excellent tool for accurate assessments of pathogen concentration dispersal in ventilated rooms as well as air velocity, pressure and temperature distributions by solving momentum, energy, species transport and turbulent energy equations. Simplified semi-analytical models are useful for determining effectiveness of *UVGI* system at low computational cost when optimizing operation of associated ventilation systems to reduce the spread of airborne bacteria. Riley and Permutt (1971) presented a two-zone model where the space is divided into two horizontal and adjacent zones where air is assumed fully mixed within each zone and is irradiated in the upper zone. The air exchange rate between the two zones was determined by using the ratio of two different *UV* intensities and corresponding disinfection rates in the lower zone. Nicas and Miller (2009) developed a three-zone model, adding a near field zone to model of Riley et al. (1971) surrounding the infection source assuming also that the near field zone is well-mixed. Noakes et al. (2004) developed analytical two-zone and three-zone mixed models with the air in each zone being fully mixed, but with incomplete mixing between the zones. The mixing coefficients between zones were determined using the

inter-zonal velocities found either by measurements or *CFD*. The model results were compared to *CFD* values and good agreement was reported for suitable mixing factors.

The aforementioned simplified models ignored the gravitational settling and deposition assuming that pathogens are carried by particles smaller than 5 μm that remain airborne for long periods of time. However, the pathogen transport may also occur via particles of larger size emitted by infected occupants. In this case, the pathogen deposition should be taken into account in the modeling to obtain accurate predictions of the pathogen dispersion and UVGI effectiveness. Habchi et al. (2014) developed a simplified model to predict the active particle behavior in *DV* spaces. They concluded that the ventilation flow rate should be sufficiently high to overcome the gravitational settling of particles and then prevent the stratification in particle concentration from occurring at the breathing level.

To our knowledge, no study has investigated the combination of *UR-UVGI* with either localizing *CC/DV* or horizontal zoning air distribution systems. Furthermore, the use of return air has not been modeled when using *UR-UVGI* in any of the *HVAC* systems.

The main target of this thesis is to investigate the applicability and efficacy of *UR-UVGI* in reducing the airborne and droplet cross infection in both vertical localization *CC/DV* and horizontal localizing air conditioning system recycling return air.

It is aimed to study using *CFD* the bacteria transport and air disinfection in *UR-UVGI* spaces conditioned by mixed localized *HVAC* systems. The potential of cross-infection is assessed based on the bacterial concentrations at the breathing level that is

compared with the *WHO* standard limit of 500 CFU/m³ of bacteria in the occupied zones.

Furthermore, a simplified model for pathogen transport and deposition at different droplet sizes in *CC/* mixed *DV* spaces is developed and experimentally validated. The simplified model is used to study the effect of the pathogen-carrying particles size on pathogen distribution and UR-UVGI effectiveness in spaces conditioned with *CC/mixed DV* systems. The model can also serve as a design tool that reasonably determines the maximal return air fraction that can be used to optimize the economic viability of the *CC/DV* system.

CHAPTER II

THE STATE OF ART OF UVGI

Ultraviolet light has been successfully used in disinfecting water and equipment since the late 1800s. Applications to indoor air disinfection began in the 1930s but had varying degrees of success. Air disinfection systems are commonly used today in health care facilities. Some limited use of UVGI for air disinfection occurs in schools and in domestic households. The largest market is hospitals, with an almost even distribution of the rest among prisons, shelters, offices, and clinics.

On the average, viruses and fungal spores are more resistant to UV inactivation than bacteria while the vegetative fungi cells are about as susceptible to UV as bacterial cells (Kowalski, 2009).

A. Indoor Bioaerosol Sources

Bioaerosols such as bacterial and fungal cells and their spores have been related for a long time to human health issues (Cole and Cook, 1998; Kearns et al., 2000, Shukla et al., 2011). Mandal and Brandl (2011), in their review article, identified commonly detected airborne microorganisms (Bacteria and Fungi) and their concentrations in various selected indoor locations. The predominant types of airborne bacteria in a general hospital were *Staphylococcus*, *Bacillus*, *Micrococcus*, and *Corynebacterium* with bacterial counts ranging from 35 to 728 CFU/m³. In schools and

offices, predominance of *Bacillus*, *Corynebacterium*, *Micrococcus*, and *Staphylococcus* were reported with bacterial count as high as 1696 CFU/m³.

Two of the major sources of airborne bioaerosols in indoor environments are: occupants and contaminated *HVAC* systems. In the current study, biological contaminants from outdoor air are not considered in *IAQ* assessment.

1. Human Expiratory Activities

Occupants continuously emit bioaerosols when talking, breathing, coughing or sneezing, and are intense emitters of infectious airborne bacteria and viruses if they are infected. Researchers experimentally investigated the flow rates of exhaled air from humans and associated microbial emission rates. Early studies of endogenous particle concentrations in exhaled air during normal breathing were performed by Fairchild and Stampfer (1987). They reported that the number of exhaled particles ranged from 0.1 to 4.0 particles/cm³. VanSciver et al. (2011) measured the velocity field of human cough using particle image velocimetry and reported maximum cough velocities between from 1.5 m/s to 28.8 m/s. Mahajan et al. (1994) found that the cough mean peak flow rate was of 300 L/min. Singh et al. (1995) found that the peak flow rate of women cough reached 750 L/min and the peak flow rate of men cough reached 1300 L/min .

Xu et al. (2012) reported concentrations ranging from 700 to 6,000 CFU/m³ of bacteria, mainly *Sphingomonas paucimobilis* and *Kocuriarosea*, in the air exhaled by human subjects with the onset of flu symptoms. Wainwright et al. (2009) reported through an experimental study that a person with Cystic Fibrosis disease produces up to 13,000 CFU/m³ of viable inhalable bacterial aerosols when coughing, mainly

Pseudomonas aeruginosa. Fennelly et al. (2004) reported that, during 5 minutes of continuous coughing, the average concentration of *Mycobacterium tuberculosis* in the cough of an infected human is 633 CFU/m³.

In addition to the flow rate and bioaerosol concentration of air exhaled from infected people, the size distribution of expiratory droplets is an important factor that greatly affects the disease transmission in indoor environments. This is due to the fact that pathogens from an infected person are carried by the saliva droplets that he emits.

Published experimental cough and sneeze droplet size distribution data showed that the emitted particles may vary in size from 1 µm to greater than 100 µm (Papineni and Rosenthal, 1997; Duguid, 1946; Loudon and Roberts, 1967). In more recent studies, interferometric Mie imaging (IMI) technique was used to determine the size distributions of expiratory droplets expelled during coughing and speaking. It was reported that the geometric mean diameter of droplets from coughing was 13.5 µm and it was 16.0 µm for speaking (Chao et al., 2009). Nevertheless, an emitted droplet can rapidly undergo a water loss to an equilibrium diameter that is approximately one-half the initial diameter (Nicas et al., 2005). Some expiratory droplets shrink in size to become “droplet nuclei” of 1 - 5 µm which sustain in air for prolonged periods of time and can reach the alveolar region of the lung. The term “droplet nuclei” was introduced by Wells (1946) as being the dried residues of expiratory droplets smaller than 100 µm; whereas the recent study of Nicas et al. (2005) showed that an exhaled droplet larger than 20 µm cannot become a “droplet nucleus”. It was identified that when pathogens are carried by droplet nuclei, the disease transmission is said to be of “airborne” mode (Centers for Disease Control and Prevention, 2003). On the other hand, pathogen-carrying particles of aerodynamic diameter between 5 and 100 µm can be either inhaled

into the head airways region of the respiratory system (Miller et al., 1979). Pathogen-carrying particles of this size or larger can also be removed from air by rapid gravitational settling and deposition onto solid surfaces, and then transferred by touch to new patients. Nevertheless, when a susceptible person is in the proximity of an infected person, a relatively large particle can be airborne long enough to be inhaled by the exposed person. This can exemplify the “droplet” mode of disease transmission.

2. Biologically Contaminated HVAC Systems

HVAC systems with no regular cleaning may carry significant amounts of bacterial aerosols and fungi and consequently supply contaminated air into conditioned spaces. Microbial contaminants in *HVAC* systems accumulate on heat exchangers and fins, in condensate drain pans, on air filters, and in air ducts. Those *HVAC* components, with their moist conditions, are considered ideal environments for bacteria and fungi to multiply and colonize (Kemp et al., 2001; Schmidt et al., 2012; Bródka et al., 2012).

Hughenoltz and Fuerst (1992) reported bacterial concentrations up to 10^6 CFU/m² on air-handling cooling coils. Researchers reported that the household air conditioning units can discharge up to 2,500 CFU/m³ of bacteria and 1,000 CFU/m³ of fungi above ambient levels on initial startup (Jo and Lee, 2008). Li et al. (2011) reported, based on actual measurements, that bacterial concentration of type *Beta Streptococcus* in air supply diffusers of *HVAC* systems, functioning normally in public places and hospitals, reached values of 1,142 CFU/m³ and 918 CFU/m³ respectively.

B. UVGI Systems

The ultraviolet wavelength range extends from 100 to 400 nm, covering the three radiation bands (short, mid and long wavelength UV radiation). Ultraviolet A (UVA) is the radiation with the highest wavelength (320 - 400 nm), UVB ranges between 280 and 320 nm, while UVC is the lowest wavelength UV radiation (100-280 nm). Low-pressure mercury lamps are commonly used in *UVGI* applications. Airborne germs are mostly susceptible to ultraviolet radiation of wavelength of 254 nm, which destroys the nucleic acids of the microorganism. The effectiveness of ultraviolet radiation in destroying infectious microorganisms is well established by many researchers. The ability of *UVGI* to efficiently inactivate airborne microorganisms was first demonstrated by Wells and Fair (1935). Wells et al. (1942) demonstrated the effectiveness of the *UR-UVGI* in reducing measles infection in schools. Furthermore, Riley et al. (1957) documented the effect of UV radiation in decreasing the concentration of TB inside enclosed spaces. The interest in the use of UV radiation for disinfection has decreased because of the discovery of antibiotics and the reduced occurrence of TB. In recent years, there has been renewed interest in UV radiation due to the emergence of drug-resistant bacterial strains, such as TB and SARS, and the need to reduce cross-contamination in crowded spaces while minimizing the energy consumption for ventilation.

1. Air Disinfection Systems

UV systems for disinfecting air will either use forced air, as with in-duct or recirculation units, or rely on natural air movement for circulation, as in upper room *UVGI* systems.

The disinfection of indoor air is mainly accomplished by three methods:

- irradiation of the whole room-air
- irradiation of the upper room-air
- in-duct irradiation of the recirculated room-air

For upper room irradiation, germicidal lamps UVGI systems can be either wall mounted or suspended from the ceiling. The bottom of the lamp is usually shielded or louvered to direct radiation upward, above a predetermined height. In-duct UVGI systems are used for disinfecting an airstream in a building or zonal ventilation system. In general, those systems consist of UV lamps, fixtures, and ballasts, and rely on filters to keep the lamps clean. UV lamp fixtures can be placed almost anywhere in the ductwork and the air handling unit.

Each of these methods has its own advantages and disadvantages. For example, using *UV* radiation inside the *HVAC* ducting systems protects occupants from direct exposure to *UV* radiation. However, this approach is not energy efficient. Air velocity in ducts is relatively high, which reduces the time for which airborne pathogens are exposed to *UV* irradiation. Then, in-duct *UVGI* systems require higher *UV* output, compared to the other types, to achieve the same bacterial killing rate. Irradiating the whole room air is very effective in disinfecting the air but not practical, as occupants are required to wear special protective clothing and goggles. On the other hand, irradiating the upper room air allows having an occupied zone with harmless *UV* irradiance levels when the *UV* lamps are appropriately installed. Ultimately, the choice of which system to use depends on both economics and installation feasibility.

2. Upper Room UV Safety

The primary safety issue concerning upper room UVGI systems is that occupants may be exposed to direct or reflected UV rays for long periods of time. UV lamps in practical applications are selected such that they meet the safety limit for UV irradiance. The permissible limit of UV irradiance in the occupied zone is $0.2 \mu\text{W}/\text{cm}^2$ based on 8 hours of continuous exposure, to prevent any occupant eye or skin injury (American Conference of Governmental Industrial Hygienists, 1999)

Many researchers have recommended that the UV lamps be installed a minimum of 2 m high (Xu et al., 2003; Noakes et al., 2006) to ensure low levels of UV irradiance in the occupied zone so that neither humans nor furniture will be affected. Nardell et al. (2008) evaluated the safety of occupants in the Tuberculosis Ultraviolet Shelter Study. They recommended that UV fixtures be installed at a height of no less than 2.13 m, and limited the irradiation in the occupied zone to $0.4 \mu\text{W}/\text{cm}^2$. On the other hand, the upper room UVGI system may always use UV lamps with louvers and shields to limit the radiation to the upper zone.

3. UV Lamp Modeling

The modeling of UVGI systems is absolutely needed when it comes to assess the UV dose, which is then used to calculate disinfection rates for specific airborne pathogens. The modeling of UV irradiance fields can be also done for the purpose of system sizing.

The UV dose received by any airborne microorganism passing through the UV field is the product of the incident irradiance and the exposure time to UV. The

irradiance field of the UV lamp can be determined through the use of thermal radiation view factors (Kowalski et al., 2003).

Ultraviolet light interacts with the materials it encounters through absorption, reflection, refraction, and scattering. Several predictive models for irradiance fields due to UV lamps have been proposed in the past (Jacob and Dranoff, 1970, Qualls and Johnson (1985), Beggs et al. (2000). The model used in the current work is an extension of Modest's model (1993) based on thermal radiation view factors, which define the amount of diffuse radiation transmitted from one surface to another (Wu et al., 2011). Their model tackles both bare and louvered linear *UV* lamps. The irradiation reflected by the room surfaces is neglected assuming diffusive enclosures. The inter-reflected intensity field is also not taken into account even between the reflectors due to their negligible area with respect to the room total area.

The irradiation reflected by the room surfaces is neglected assuming diffusive enclosures. The louvered lamp and reflector setting is approximated by a fictitious rectangular surface which is perpendicular and adjacent to the louvers. The *UV* intensity generated by the surface depends on the reflector and lamp conditions. It will be evaluated by:

$$E_s = fE_{UV} \quad (1)$$

where f is the reflectivity of the lamp reflector and E_{UV} is the lamp power input.

Therefore the UV power output is be divided across all louvered lamp sub-surfaces as follows:

$$E_s = H_s L_s \sum_i I_{s,i} \quad (2)$$

where H_s, L_s are the fictitious surface height and length respectively and $I_{s,i}$ is the intensity of the sub-surface i corresponding to the i^{th} slot.

It is assumed that each surface i of area $A_{s,i}$ has the same sub-intensity:

$$I_{s,i} = \frac{E_s}{A_{s,i}} \quad (3)$$

Next, the view factor between a given differential surface in space and a sub-surface i will be calculated. Three zones in space depending on the range in which the sub-surface can be seen at the point $P(x,y,z)$ through the louvers and the valid UV irradiation source of the sub-surface is calculated accordingly.

4. Measuring UV Irradiation

There are two basic methods to measure the intensity of UV irradiation: radiometry and actinometry. Radiometry measures irradiance, the UV energy striking a surface from all forward directions expressed as energy (watts) per unit area. A radiometer is a sensor with an electronic readout device that displays the sensor readings.

Actinometry is the second method of measuring UV irradiation. Actinometry is based on chemical systems that undergo light-induced reactions at specific wavelengths for which the quantum yield is accurately known (Kuhn et al., 2004). This method has application for those situations in which UV radiation from more than one direction or source impinges on a three-dimensional object, and when it is of interest to determine the radiant fluence experienced by the object. The radiant fluence is defined as the total radiant power incident from all directions onto the object.

5. UVGI Efficacy Evaluation

The effectiveness of the *UV* device in inactivating a particular microorganism is described using the killing rate (disinfection rate) given by:

$$KR = 1 - S \quad (4)$$

where *S* is the microorganism survival rate, *S*, defined by:

$$S = \frac{C_{UV}}{C_0} \quad (5)$$

C_0 and C_{UV} are respectively the concentrations of viable microorganisms before and after *UV* exposure (Sung and Kato, 2010; Sandberg and Sjoberg, 1983), D_{UV} is the *UV* dose received by the microorganism and *Z* is the susceptibility of the microorganism to *UV*. The susceptibility of bioaerosols to *UV* can be defined by the *UV* exposure dose (fluence) required for 90% inactivation.

6. Factors on UR-UVGI Performance

The success of air disinfection by upper room irradiation greatly depends on the *UV* intensity and distribution above the heads of occupants and on the vertical air movement between the lower occupied zone and the upper irradiated zone.

Sung and Kato (2010) developed, using the concept of ventilation performance, two numerical methods to investigate the germicidal performance of *UR-UVGI* systems. They found that the design of *UR-UVGI* and ventilation openings is important for optimizing the germicidal performance.

An important factor that affects the disinfection rate of any *UVGI* system is the sensitivity of the bacteria to *UV* light. This property is known as the bacteria susceptibility to *UV* irradiation and defined by the *UV* fluence required for 90% inactivation (Kowalski et al., 2009). *Escherichia coli*, *Serratia marsescens*,

Staphylococcus aureus, *Mycobacterium bovis BCG*, *Mycobacterium tuberculosis*, and *Mycobacterium parafortuitum* are common bacteria types and of the most susceptible to UV. Therefore, they were frequently used in the literature when studying the UVGI systems.

The room conditions and ventilation were proven to affect the efficiency of UVGI (Xu et al., 2003; First et al., 2007; Ko et al., 2000; Peccia et al., 2001) experimentally proved that microorganisms are less susceptible to UV light at higher relative humidity, and thus UVGI is less effective at high humidity. Bacteria with lipid envelop are more stable in moist air where evaporation is not likely to occur. Therefore, UV susceptibility (*Z*) of bacteria decreases at high relative humidity and the UV inactivation accordingly as well. Hatch and Wolochow (1969) reported that RH of 40 to 60% has the highest lethal effect on airborne bacteria. Riley and Kaufman (1972) reported that the killing rate of UVGI system for *S.marcescens* declined drastically at RH above 80%. Miller et al. (1999) reported that inactivation rates for *M. parafortuitum* decreased by a factor of 2 when the relative humidity increased from 50% to 90%. Peccia et al. (2001) experimentally showed the decrease of *Z*-values while the relative humidity was increasing. They concluded that there is a significant decrease in airborne bacteria inactivation rates induced by UV irradiation at RH levels in excess of 50%.

However, many previous studies showed that the relationship between RH and UV susceptibility is species-dependent and no definitive general correlation can be established (VanOsdell and Foarde, 2002; Kowalski et al., 2003). In general, the room ventilation rate, temperature, and humidity play a major role in survival and growth of microorganisms.

C. Upper Room UVGI with Localized Air-Conditioning Systems

The dispersion of bioaerosols in indoor environments greatly depends on the air distribution system (Lindsley et al., 2012). Convective mixing systems result in spreading airborne pathogens and then increase the potential cross-infection among all occupants in the conditioned space. In contrast, the localized air-conditioning systems divide the conditioned space into environmental zones with minimal mixing between the adjacent zones.

1. Horizontal Localizing Air Distribution System

Horizontal air localization HVAC systems include a peripheral angled four-sided ceiling diffuser which forms a canopy for localizing air flow around the targeted occupied zone and a central return vent.

An environmental zone is eventually localized by the supply jets from the ceiling unit. This air distribution system focuses on improving microclimate comfort and IAQ of regions in the localized space instead of the whole space as needed particularly in large office spaces and workplaces with processes exposing workers and others to airborne contaminants (Kayumba et al., 2009; Cho et al., 2011). Lo and Novoselac (2010) used localized air flow distribution system to divide an open cubicle office into thermally and pollutant independent virtual zones without solid partitions. Savings of 12% on total cooling energy were reported to be achieved while providing better IAQ.

Localized air conditioning systems have been tested for their effectiveness in localizing the air conditioning needs of occupants in a given zone (Oh et al., 2014; Wang et al., 2014; Lo and Novoselac, 2010). However, this characteristic will also

localize the infectious particles in the presence of an infected person within the localized zone and hence increase the chance of cross-infection inside this zone. This leads to having to increase ventilation requirement to meet acceptable microbiological air quality which would result in higher cooling load and energy consumption. For that reason, several methods have been introduced to disinfect supply air in the duct or in the space. In-duct methods include the use of high performance air filters to trap bacteria or the use of high intensity ultraviolet (*UV*) irradiation lamps to inactivate bacteria. These methods are effective but still impose additional energy costs associated with increased pressure drop across the filters (Joubert et al., 2011) and increased *UV* intensity to compensate for the short residence time of air in ducting system (Beggs et al., 2000; Kujundzic et al., 2007). In-space method such as upper-room *UVGI* presents an alternative less costly method for cleaning the air especially when having air circulation that drives air to reside long enough in the upper zone of the room to be exposed to *UV* irradiation (Sung and Kato, 2010; Bolashikov et al., 2009; First et al., 2007).

2. Vertical Localizing Air Distribution (*CC/DV*) System

One of the HVAC systems known to provide good indoor air quality is the combined chilled ceiling (*CC*) displacement ventilation (*DV*) system which is suitable for applications when cooling load is less than $100\text{W}/\text{m}^2$ (Behne 1999). This system provides vertical air localization since it moves air from the lower occupied zone to the upper recirculated zone. It is not then suitable to combine with upper room *UVGI* when supply air is 100% fresh air because there is no mixing between the lower and upper zones, and upper-room infected air is exhausted (Keblawi et al., 2009; Ghaddar et al., 2008; Ghali et al., 2007). The 100% fresh air in the occupied zone of the *CC/DV*

conditioned room exceeds the minimum acceptable ventilation requirements of the space (ASHRAE Standard 62.1-2014). Several researchers reported that the *CC/DV* system consumed much less cooling energy than the conventional system at 100% fresh air system, but it did not offer energy savings when compared to mixed conventional systems (Bahman et al., 2009; Yuill et al., 2008; Nielsen, 2007). In humid climates, the *CC/DV* system may not be also cost effective since outdoor humidity is a major contributor to decrease the efficiency of the system since the *CC/DV* system requires relatively dry supply air to ensure that no condensation takes place at the chilled ceiling. Using mixed supply air in the *CC/DV* system is shown to improve energy performance by 20% when mixed return air ratio is about 40% while keeping acceptable CO₂ concentration of 700 ppm at the breathing level of the conditioned room (Chakroun et al., 2011; Kanaan et al., 2010). However, a decrease in CO₂ level or keeping it within the acceptable range may not ensure that the concentration of infectious airborne bacteria set at maximum allowable value of 500 CFU/m³ for offices is achieved. The level of generation of airborne bacteria might be high and require more frequent replenishment of room air than that required for CO₂. Since the *CC/DV* system relies on the *DV* system and buoyancy to drive the air upwards, then the use of *UVGI* with **mixed** *CC/DV* might be an attractive and viable option to disinfect air and reduce the spread of airborne bacteria generated by the occupants through air and surface deposition. The recirculation of the airborne bacteria in the upper room will increase its time of exposure to *UV* in the irradiated zone which results in high effectiveness for the upper-room *UVGI*.

In this work we will start by stating the specific thesis objectives in chapter 3 followed by the research methodology in chapter 4. The methodology is divided into four

parts: 1) CFD methods and validation; 2) simplified model and its validation; 3) energy performance study; and 4) experimental methodology. The CFD methods are described in Chapter 5. The experimental facilities and methods are described in Chapter 6. Chapter 7 tackles the simplified mathematical modeling of the pathogen transport and UR-UVGI performance in horizontal localization air-conditioning systems. Results and discussion are shown in Chapter 8, and finally Chapter 9 is dedicated for conclusions and future work.

CHAPTER III

OBJECTIVES AND SCOPE

A. Objectives

This thesis work aims to study by modeling and experimentation the performance of *UR-UVGI* systems in providing healthy *IAQ* in both vertical localization mixed *CC/DV* and horizontal localizing air conditioning system recycling return air. The use of *UVGI* would allow increasing the return air fraction while keeping bioaerosol concentrations below the standard limit, and then achieve significant energy savings.

B. Scope

The scope of this work includes the following steps:

- To achieve horizontal and vertical localization to minimize energy consumption by avoiding the conditioning of unoccupied zones and excess in ventilation rates.
- To determine by CFD and mathematical modeling the distribution of pathogens in both horizontal and vertical air localization systems.
- To model the use of return air for reducing the thermal load of fresh air supplied to locally conditioned spaces and evaluate the associated energy savings on the used localized air conditioning systems.

- To investigate the effect of recirculating return air on the microbiological air quality in the spaces conditioned using both horizontal and vertical air localization. The study will consider the bacteria concentration lumped for the whole horizontal breathing air region and not the immediate inhalation zone of the occupant.
- To evaluate by modeling the efficacy of UR-UVGI in preventing cross-infection in both systems.
- To test experimentally the effectiveness of UR-UVGI in disinfecting air in vertical localization (CC/DV) systems.
- To study the gravitational settling and deposition effects on the pathogen distribution and the effectiveness of UR-UVGI in CC/DV systems.
- To provide a design tool for finding the optimal return air fraction that minimizes the energy consumption of the vertical localization system (CC/DV) while meeting the *IAQ* requirements.

This work is the first to tackle the combination of *UR-UVGI* with mixed-air *CC/DV* and horizontal localizing air-conditioning systems recycling the return air and investigate the cross-contamination within one localized environmental zone.

CHAPTER IV

RESEARCH METHODOLOGY

The transport and deposition of pathogens in spaces conditioned by horizontal and vertical (CC/DV) localizing air flow with and without upper room *UV* fields are simulated using *CFD* modeling and experimentation. The horizontal localization (zonal) air distribution is shown in Fig. 1a. The localized air system will establish cool air curtain surrounding the occupied zone and will withdraw air return air from the center of the curtained zone to the upper zone. This system insures that air from the conditioned region in the space is returned to the ceiling to prevent the spreading-out of the supply jets and then maintain the localization. Fig. 2b shows the vertical air localization established by the buoyancy-driven air flow in the CC/DV system. The air contaminants are transported to the upper recirculation zone leaving the lower zone at acceptable thermal comfort and air quality.

To assess the performance of the integrated *UVGI* with the considered localized air distribution systems, 3-D detailed *CFD* model is developed using *ANSYS* 14.5 to investigate the flow, thermal, and species concentration fields associated with each of the horizontal and vertical air localization systems. The Eulerian approach is used in modeling the airborne dispersion of pathogens and the performance of UR-*UVGI*. The gravitational settling is reasonably neglected since the pathogen-carrying particles in the airborne mode of disease transmission are droplet nuclei (1 - 5 μm) whose transport is mainly governed by the airflow. Furthermore, in CC/DV systems the pathogen deposition on walls and surfaces is also neglected due to the upward and relatively low

DV airflow. On the other hand, the CFD modeling of transport and deposition of pathogens at large particle size ($> 5\mu\text{m}$) in CC/DV systems are simulated using the Lagrangian method.

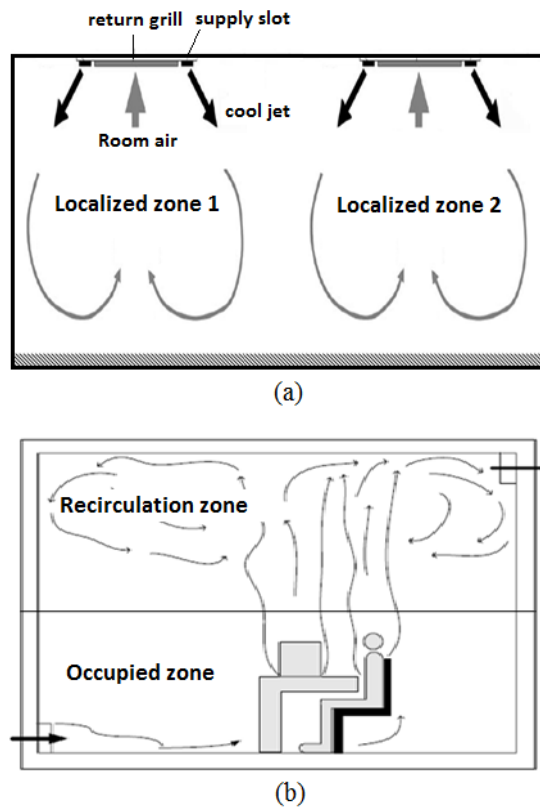


Fig. 1: Illustrations of (a) horizontal localization (zonal) airflow and (b) vertical localization in CC/DV system.

The microorganism simulated in the horizontal air localization is *Staphylococcus aureus*, which is a common bacteria type (Mandal and Brandl, 2011). Staphylococci are gram-positive bacteria with diameters of $0.5 - 1.5 \mu\text{m}$ (Harris et al., 2002). On the other hand, *Serratia marcescens* with higher sensitivity to *UV* was selected for the model of vertical air localization.

S. marcescens is an airborne gram-negative bacterium that has the shape of rods with $0.5-1 \mu\text{m}$ diameter and length less than $2 \mu\text{m}$ and might cause nosocomial infections. This bacteria type is widely used in UVGI research because of its abundant

presence in the environment and high sensitivity to *UV* (Riley and Kaufman, 1972; Lai et al., 2014; Ko et al., 2000). The typical mass of one bacterium is approximately 10^{-12} g (Davis, 1973).

Measurements are made in the simulated rooms to obtain the accurate supply and boundary conditions to be used in the simulations. The obtained airflow and thermal fields are then validated by experimentation as well.

The *UV* irradiance distribution is determined using the predictive model of Wu et al. (2011) and validated using actinometrical measurements. The validated *UV* field is incorporated with the *CFD* code through a supplementary program called user-defined function (udf). Another user-defined function is used to simulate the bacteria deposition. The integrated *CFD-UV* model is validated by experimentation and using published experimental data.

The validated *CFD-UV* model is then used to perform a parametric study of UR-UVGI effectiveness in enhancing the microbiological air quality in horizontal air localization systems and the use of return air for minimizing cooling energy consumption. The simulation parameters are the return air mixing ratio and *UV* output delivered to the space. The *UVGI* effectiveness is determined by comparing the bacterial concentrations before and after the use of *UV*.

The *CFD* predictions of airborne bacteria concentration in the simulated *CC/DV* space are validated by air sampling, whereas the bacteria deposition predictions are validated using settling petri plates. After this, a simplified mathematical model is developed to predict, at low computational cost, the pathogen transport and deposition at different droplet sizes in *CC/DV* spaces with UR-UVGI. The model is validated experimentally for pathogen-carrying particles of droplet nuclei size and then

substantiated using CFD modeling for large particles. Finally, a case study of each of the localized air conditioning systems is presented where the UR-UVGI efficacy and energy performance are evaluated using the developed models.

The methodology flow chart is shown in Fig. 2 where the research methods include three major components; 1) CFD modeling, 2) experimental validation methods of air quality and *UVGI* effectiveness, and 3) Simplified mathematical modeling.

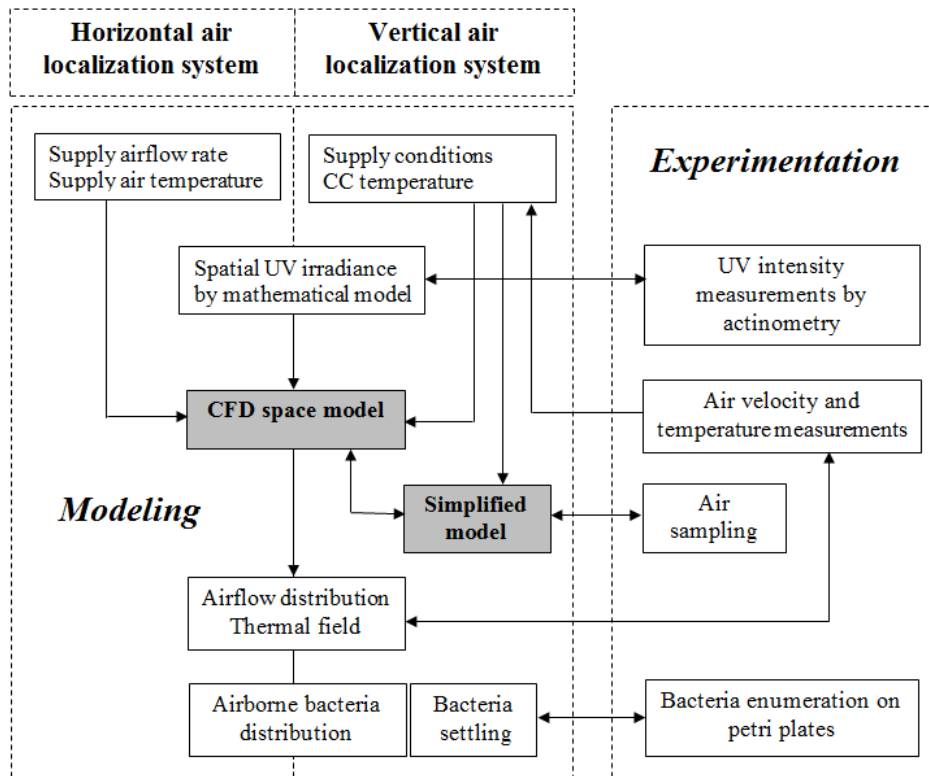


Fig. 2: Flow chart of the inputs and predicted outputs of the various models.

This work consists of the following parts:

- CFD modeling, using Eulerian methods, of the airborne dispersion of pathogens and efficacy of UR-UVGI in both horizontal and vertical air localization systems.

- CFD modeling, using Lagrangian tracking, of the transport and deposition of pathogens at large droplet sizes.
- Experimentation to obtain accurate airflow and thermal boundary conditions to be used in the CFD simulations for both horizontal and vertical air localization systems. Experimental data is also used to validate the developed CFD models.
- Validation of the developed CFD-UV model using published experimental data.
- Parametric study using the validated CFD-UV model to determine the optimal return air mixing ratio in horizontal air localization systems with and without the use of UR-UVGI. The associated energy performance is also evaluated.
- Simplified mathematical modeling to determine the distribution of the airborne pathogens (gravitational effects are neglected) and the optimal return air mixing ratio at minimal computational cost. The predictions of the developed simplified model are compared with the results of the experimentally validated CFD model.
- Implementing the simplified model on a case study to determine the return air mixing ratio that maximizes the energy consumption while maintaining acceptable IAQ in the breathing air layer with and without the use of UR-UVGI.
- Extending the simplified mathematical model to encompass different droplet sizes in simulating the dispersion of pathogens and UR-UVGI effectiveness in CC/DV rooms. Here, the pathogens may be carried by active particles ($> 5 \mu\text{m}$) and then the gravitational settling and deposition are taken into account for accurate predictions of pathogen distribution.
- Experimental validation of the extended mathematical model using small droplets. The airborne pathogen concentration is measured at different locations using air sampling. The settling of pathogens is also measured using settling

petri plates on which the pathogen colony forming units are counted after incubation.

- CFD modeling using Lagrangian particle tracking stochastic model to determine the distribution of airborne pathogens and accurately predict the gravitational settling and deposition. Particle size is an important parameter in the simulations. The CFD predictions of pathogen deposition at small particle size are validated using experimental CFU counts.
- CFD substantiation of the mathematical model for large pathogen-carrying particles. The airborne pathogen distribution predicted using the mathematic model is compared with the predictions of the experimentally-validated CFD model.
- Use of the validated mathematical model to study the effect of droplet size on the pathogen transport and UR-UVGI efficacy in chilled ceiling and mixed displacement ventilation systems.

CHAPTER V

CFD METHODS

It is important to use detailed *CFD* models that can accurately predict the angled jet entrainment and mixing in the horizontal air localization system and the entrainment and mixing between the plume and the surrounding in the vertical air localization system (CC/DV). The gravitational settling and deposition should also be reasonably predicted. Therefore, proper modeling of flow physics is critical: turbulence models, buoyancy effects, and boundary layers. The use of experimentally obtained boundary conditions is also essential for accuracy of numerical predictions (Srebric and Chen, 2002).

Two pathogen modeling methods including the Eulerian and Lagrangian methods have been used in the literature. The Eulerian method treats the particle phase as continuum, whereas the Lagrangian method considers particles as a discrete phase and tracks the path line of each individual particle. Throughout the literature review, both of the methods can well predict the particle concentration under steady-state conditions, but the Lagrangian method is computationally more demanding (Heidarinejad and Srebric, 2013; Hathway et al. 2011). On the other hand, the Lagrangian method shows superiority in simulating large particles and unsteady particle sources (Zhao et al., 2004, 2005; Zhang and Chen, 2007; Mui et al., 2009).

To our knowledge, the simulation of recirculating the return air is not feasible in the Lagrangian method since particles cannot be tracked anymore or returned back into the computational domain after escaping from it. Thus, we will use the Eulerian

approach to simulate the transport of pathogens in the mixed air localization systems (Noakes et al., 2006; Sung et al., 2009; Sung and Kato, 2010). The return air recirculation is modeled using a user-defined interpreted by the CFD software. Nevertheless, the Lagrangian method will be used to predict more accurately the gravitational settling and deposition of pathogens

Steady-state *CFD* simulations of the test rooms are carried out using the commercial software ANSYS 14.5 and selecting the momentum method for air diffuser simulation. The environmental setup including supply, exhaust, microorganism source, and the *UVGI* lamp sizes and positions is kept as close as possible to the real environment. However, there are discrepancies between the experimental setup and *CFD* simulations due to pieces of missing information. The air flow is simulated using the standard $k-\varepsilon$ turbulence model which is known to produce valuable, accurate and experimentally validated results (Wan and Chao, 2005). The airborne transport of pathogens is simulated using Eulerian approach and the droplet transport and deposition are simulated using Lagrangian approach.

A. Flow and Thermal transport

The simulations of both horizontal air localization room and CC/DV room are carried out using a tetrahedral grid containing sufficient number of cells to ensure grid independence, refined around the boundaries and species sources (Fig. 3). Horizontal circular surfaces are introduced and defined as walls in the computational domain to simulate the petri plates that will be used in the experiments to measure the pathogen deposition in the CC/DV space.

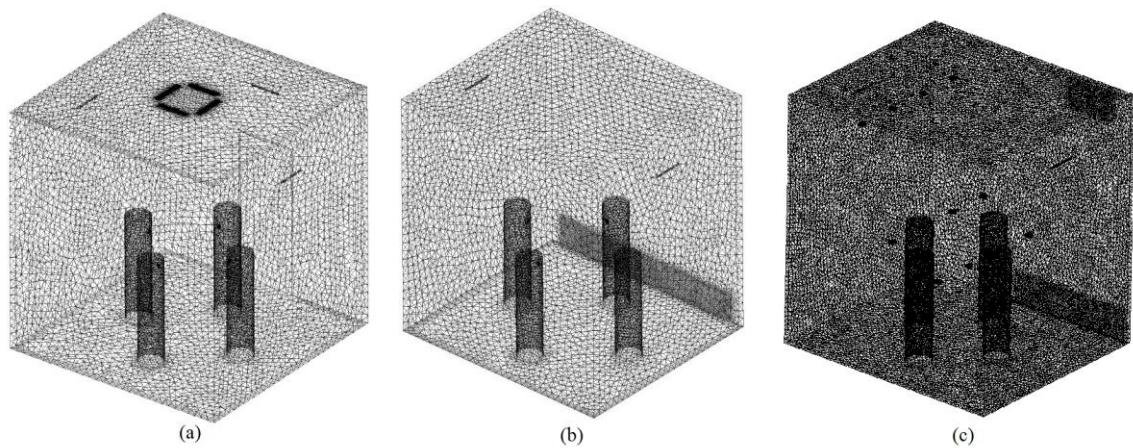


Fig. 3: Grids generated by ANSYS mesher for the (a) horizontal localizing air flow room (1,500,000 elements) and vertical air localization (CC/DV) room for (b) Eulerian simulations (1,270,000 elements) and (c) Lagrangian simulations (1,700,000 elements).

Pressure outlet boundary condition is imposed at the exhaust. A standard k- ϵ turbulence model is used with a no slip condition applied at the walls. To account for the thermal buoyancy, the “Boussinesq” approximation is used for the buoyancy-driven flow assuming small density differences in the room air. To simulate the pathogen deposition on the walls of the horizontal air localization room, the option of “standard wall function” is activated requiring the y^+ to be within 30 and 300 (Ariff et al., 2009; Chmielewski and Gieras, 2013). This is to ensure adequate meshing of the wall turbulent boundary layer containing the particle deposition boundary layer (Lai and Nazaroff, 2000). Moreover, radiation is neglected in horizontal air localization system since there are no significant temperature differences between the internal walls’ surfaces.

All variables, except the pressure, are discretized with the second-order upwind scheme. STANDARD scheme is used for the pressure term and the SIMPLEC scheme with skewness correction 5 is used for coupling pressure and velocity. It is important to

ensure that the numerical results are stable and converged and do not exhibit transient behavior due to instabilities in the buoyant flows. To obtain a valid steady state solution in presence of buoyancy forces, the under-relaxation factors are manipulated to dampen the flow oscillations that may arise. Convergence is defined when residuals are less than 5×10^{-5} and the net fluxes of mass and heat are less than 1%.

Additionally and in order to make sure that our assumption that the localized air-conditioning system offers zonal protection as has been reported by Lo and Novoselac (2010), the bioaerosol confinement analysis is performed by simulating a space with two localized identical air zones. The same modeled space is doubled in size to have two identical and symmetrical flow and thermal zones. The only difference between the two localized zones is that one of them has two bacteria-emitting cylinders and the other one has no bacteria emissions. Same features of the CFD model are used for a mesh containing around 8,200,000 elements.

B. Bacteria Transport and UV Inactivation

The *CFD* model will help to assess the *IAQ* by determining the bacteria concentration in the air surrounding the occupants lumped in the breathing layers and not the “breathing zone” defined in ANSI/ASHRAE Standard 62.1-2014. The contaminant concentration in the micro-inhalation zone will not then be considered.

Therefore, the representation of the complex geometry of the face or other parts of the human body is not required in the proposed CFD simulations. It would be then reasonable to simulate humans by cylinders to reduce mesh size and computational cost (Lo and Novoselac, 2010; Dunnett, 1994). Occupants are then simulated by heated cylinders of diameter 0.3 m and height 1.2 m each having a heat load of 100 W. Each

cylinder has a circular hole of area 1.2 cm² at height 1.05 m that simulates human mouth emitting 0.6 L/min of CO₂ at 34°C. Infected occupants are assumed to generate *S. aureus* or *S. marcescens* at rate 700 CFU/min each

1. Eulerian Model

The Eulerian method is used to simulate the airborne transport of pathogens and the inactivation of microorganisms due to *UV* irradiation in both horizontal and vertical air localization systems. The *CFD* code will solve the following transport equation (Noakes et al., 2004; Hathway et al., 2011)

$$\nabla \cdot [(U + V_s)C] - \nabla \cdot [(D + D_t)\nabla C] - Z \times E \times C = 0 \quad (6)$$

where *U* is the air velocity field, *V_s* is the settling velocity of pathogen-carrying particles, *C* is the microorganism concentration, *D* is the Brownian diffusivity, *D_t* is the particle Eddy diffusivity. The last term, *Z*×*E*×*C*, in Eq. 6 is a spatial sink term that represents the rate of inactivation due to the *UV* field where *E* is the *UV* irradiance at the centroid of a grid cell, and *Z* is the microorganism susceptibility to *UV*. The *UV* susceptibilities of *S. marcescens* and *S. aureus* are respectively 0.57 m²/J (Ko et al., 2000) and 0.35 m²/J (Sharp, 1940) at RH between 40 and 60%.

The majority of particles emitted by normal breathing are much smaller than 20 μm (Morawska, 2006; Papineni and Rosenthal, 1997). These particles evaporate within a few milliseconds to become droplet nuclei (1 - 5 μm) that sustain in air for long periods of time. It was also reported by Bourouiba et al. (2014) that expiratory droplets less than 50 micrometers in size can frequently remain airborne long enough to reach ceiling ventilation units.

The gravitational settling is then reasonably neglected. Pathogen deposition is also neglected in the CC/DV system due to the upward DV flow. On the other hand, the deposition of particles on walls is enhanced by the downward supply jets of the horizontal air localization system and then cannot be neglected. The particle wall flux is determined with a one-dimensional semi-empirical particle deposition model (Lai and Nazaroff, 2000).

The spatial distribution of *UV* irradiance in the modeled space is determined using the model of Wu et al. (2011) for bare and louvered *UV* lamps. The irradiation reflected by the room surfaces is neglected assuming diffusive enclosures. The predicted *UV* field is incorporated to the *CFD* code through a user-defined function (udf) written in C++ to compute the *UV* irradiance intensity at the centroid of each grid cell.

The developed CFD-UV is then validated using published experimental work of Macher and Miller (2000) in which they experimentally investigated the efficacy of upper-room *UVGI* in inactivating three types of airborne bacteria: *B. subtilis*, *E.coli*, and *M. Luteus* at steady-state conditions.

To simulate the return air recirculation in the air distribution system, an additional user-defined function is developed and incorporated to the *CFD* code to represent the following species boundary condition at the supply:

$$C_{supply} = xC_{exhaust} + (1 - x)C_{outdoor} \quad (7)$$

where x is the return air mixing ratio. It is assumed that the air filter in use is of MERV 1 efficiency. This typical filter is inefficient in capturing particles smaller than 5 μm (ASHRAE Standard 52.2-2012) and is used for conservative assessment of microbial IAQ. The outdoor bacteria concentration is neglected.

The deposition of bacteria is neglected for the horizontal air localization system

except on the room walls where the deposition of bacteria-carrying particles may be significant due to downward and angled supply jets.

To account for the bacteria deposition effect, the nominal concentration on a vertical wall is defined as (Gao and Niu, 2007) :

$$C_{wall} = C_{cell} - C_{cell} U_d \frac{\delta y}{D + D_t} \quad (8)$$

where C_{wall} is the nominal particle concentration on a vertical wall that serves as the boundary condition for Eq. 6, C_{cell} is the concentration in the near-wall grid cell beyond the concentration boundary layer, δy is the distance between the grid cell center and the wall, and U_d is the particle deposition velocity that is calculated as follows (Lai and Nazaroff, 2000):

$$U_d = \frac{u^*}{I} \quad (9a)$$

where u^* is the friction velocity and I is an integral number defined as:

$$I = 3.64Sc^{2/3}(a - b) + 39 \quad (9b)$$

The two numbers a and b are evaluated as follows:

$$a = \frac{1}{2} \ln \left[\frac{(10.92Sc^{-1/3} + 4.3)^3}{Sc^{-1} + 0.0609} \right] + \sqrt{3} \arctan \left[\frac{8.6 - 10.92Sc^{-1/3}}{10.92\sqrt{3}Sc^{-1/3}} \right] \quad (9c)$$

$$b = \frac{1}{2} \ln \left[\frac{10.92Sc^{-1/3} + r^+}{Sc^{-1} + 7.669e^{-4}(r^+)^3} \right] + \sqrt{3} \arctan \left[\frac{2r^+ - 10.92Sc^{-1/3}}{10.92\sqrt{3}Sc^{-1/3}} \right] \quad (9d)$$

Sc is the Schmidt number and r^+ is defined as:

$$r^+ = \frac{d_p u^*}{2\nu} \quad (9e)$$

where d_p is the particle diameter and ν is the kinematic viscosity of air.

The boundary conditions for the simulations are summarized in Table 1

Table 1: Boundary conditions of the simulations.

	Vertical air localization (CC/DV) system		Horizontal air localization system (Eulerian method with deposition)
	Eulerian, no deposition	Lagrangian, with deposition	
Room air inflow	U = 0.15 m/s, Turbulent intensity: 5.5%, T = 20.44°C		U = 1.93 m/s, Turbulent intensity: 9.2%, T = 16.2°C
Room air outflow	Pressure outlet		Pressure outlet
CC temperature	T = 18.05°C, no slip		-
Room walls	T = 22.09°C, no slip		T = 24°C, no slip, nominal particle concentration for bacteria
	“zero-flux” for species	“Trap” for particles	
Heated cylinder	$\Phi = 100$ W, no slip		$\Phi = 100$ W, no slip, nominal particle concentration for bacteria
	“zero-flux” for species	“Trap” for particles	
Mouth	Opening area 1.2cm ² , q _b = 700 CFU/min (<i>S. aureus</i>) q _c = 0.6 L/min, T = 34°C		Opening area 1.2cm ² , q _b = 700 CFU/min (<i>S. marcescens</i>) q _c = 0.6 L/min, T = 34°C
Lighting	Typical load: 12 W/m ²		Typical load: 12 W/m ²

2. Lagrangian Tracking Model

Lagrangian Particle tracking with stochastic discrete random walk (*DRW*) model is used to represent the Eddy interactions of the discrete phase. Throughout the literature review, this model can well predict the transport and dispersion of particles and bioaerosols in indoor environments (Hathway et al., 2011; Heidarinejad and Srebric, 2013).

Pathogen-carrying droplets are simulated as inert spherical particles, 2.5µm in diameter, with density of 1000 kg/m³. In this method a large enough number of 100,000 particles are tracked in the simulations to ensure accurate predictions of the stochastic model. Particle trajectories are calculated by a fifth order Runge-Kutta method by

considering the change in particle velocity u_p due to drag force, inertia $(u - u_p)$, lift force F_L and Brownian motion $n(t)$ thus:

$$\frac{du_p}{dt} = \frac{1}{\tau} \frac{c_d \text{Re}_p}{24} (u - u_p) + g + F_L + n(t) \quad (10)$$

where τ is the particle relaxation time given by:

$$\tau = \frac{\delta d_p^2 c_s}{18\nu} \quad (11)$$

where δ is the particle-fluid density ratio, ν the fluid kinematic viscosity and c_s is the Cunningham-Stokes slip correction factor given by:

$$c_s = 1 + \frac{2\lambda}{d_p} \left(1.257 + 0.4 \exp\left(-\frac{1.1d_p}{2\lambda}\right) \right) \quad (12)$$

where λ is the gas molecular mean free path.

The deposition of bacteria is simulated using “trap” boundary condition on the walls and other surfaces in the domain.

The three dimensional predictive *UV* model of Wu et al. (2011) is used to integrate the *UV* irradiance field into *CFD* simulations. Local *UV* intensities are implemented into *CFD* control volumes during the post-processing stage. Then, based on the residence time of each particle provided by Lagrangian tracking and the *UV* susceptibility of the microorganism, the received *UV* dose received by each particle is computed as being the *UV* irradiance multiplied by the residence time. A pathogen-carrying particle is deleted when the integrated *UV* dose it has received can achieve bacterial disinfection rate of 90%. This local *UV* irradiance intensity model for bacteria inactivation is performed by developing a user-defined function that is compiled by the *CFD* software.

Chapter VI

Experimental Methods

Experiments are carried out in two climatic rooms equipped with *UR-UVGI* systems. One of the rooms is conditioned by *CC/DV* and the other uses the zonal air conditioning system. Air velocity and temperature measurements are made in the rooms to determine accurate supply conditions to be used in the simulations and then validate the numerical predictions of air flow and thermal fields. The bacteria generation and measurements are made only in the *CC/DV* room that is equipped with high-efficient particulate matter (HEPA) filters. This experimentation aims to measure the airborne bacteria concentration in an experimental *CC/DV* to validate the simplified mathematical model of pathogen transport and inactivation with *UVGI*. The bacteria deposition in the *CC/DV* space with and without the use of *UVGI* is also measured using settling petri plates to validate the predictions of the CFD model using Lagrangian approach.

A. Room with Horizontal Air Localization System

The experimental *UVGI* room, conditioned by horizontal localized air flow by using multiple peripheral slot diffusers and a central return vent, is shown in Fig. 4. The dimensions of the room are 2.80 m × 2.80 m × 2.77 m. The conditioned air is supplied through the four supply slots of a cassette-type unit with dimensions 0.36 m × 0.04 m each, and exhausted through a 0.33 m × 0.33 m return vent.

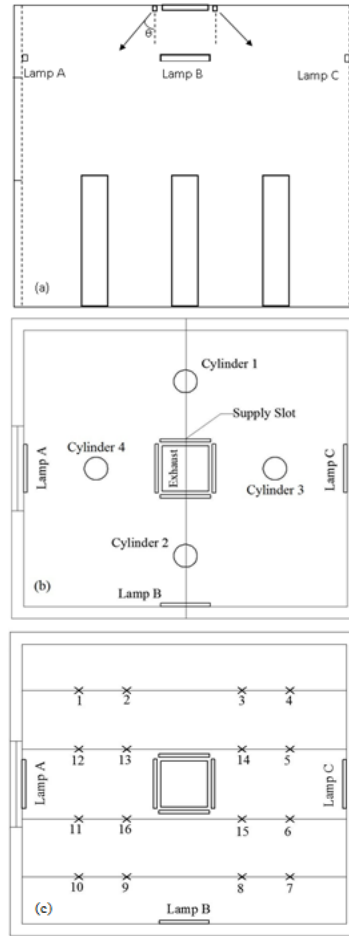


Fig. 4: Schematics of the climatic room (a) side view, (b) top view, and (c) top view showing the positions of actinometrical measurements

The supply jet angle, speed and temperature are controllable by the design of the cooling ceiling unit. The used supply conditions should provide thermal comfort and satisfy the ventilation requirement of 10 L/s per person. Four heated cylinders each of 0.3 m diameter and 1.2 m height are present in the room. The heat output of each cylinder is 100W representing the sensible load from the occupant and its personal equipment. Each cylinder is attributed with a constant generation of 0.6 L/min of CO₂ at 34 °C. Two of the cylinders represent infectious cases with a constant generation of

1,400 CFU/min of *S.aureus* by breathing, talking and coughing (VanSciver et al., 2011; Gutierrez, 2011; Wainwright et al., 2009). The lighting load is typical of 12 W/m².

The *UR-UVGI* system consists of three louvered linear low-pressure mercury lamps with 18 UVC W output, 35.6 cm length and 1.54 cm diameter each (Dinies, Germany). The lamps are mounted horizontally on three different walls at a height of 2.3 m from the floor.

B. Room with Vertical Air Localization (CC/DV) System

The schematic of the CC/DV test room is shown in Fig. 5. It is a 2.75 m × 2.5 m × 2.8 m room located in a conditioned space at 24°C and equipped with a *UVGI* system consisting of two louvered 18W UVC lamps of length 35.6 cm and diameter 1.54 cm diameter (Dinies, Germany) installed at a height of 2.5 m. The test room is equipped with a mechanical ventilation system that can deliver up to 0.2 m³/s of high efficiency particulate air (HEPA) filtered outdoor air through a rectangular grill near the floor level. A negative pressure of about 20 Pa is maintained inside the room. The chilled ceiling is composed of three copper tube and plate panels that cover the whole room ceiling area. The chilled water is supplied in parallel to the headers of each panel. The chilled ceiling temperature is controlled using an electric heater. Two 3-way control valves are implemented in the supply line to control panel temperature and inlet water temperature to the fan coil unit that cools supply air from outdoor environment to the desired supply value. The supply conditions should satisfy the CC/DV charts for thermal comfort and acceptable *IAQ* (Ghaddar et al., 2008).

The room contains four occupants of whom two are infected. Occupants are simulated by heated cylinders of diameter 0.3 m and height 1.2 m each having a heat load of 100 W and emitting 0.6 L/min of CO₂ at 34°C. Infected occupants are assumed to generate *Staphylococcus aureus* by breathing and talking at the rate of 700 CFU/min each (Nielsen et al., 2009; Fairchild and Stampfer, 1987). The lighting load is typical of 12 W/m².

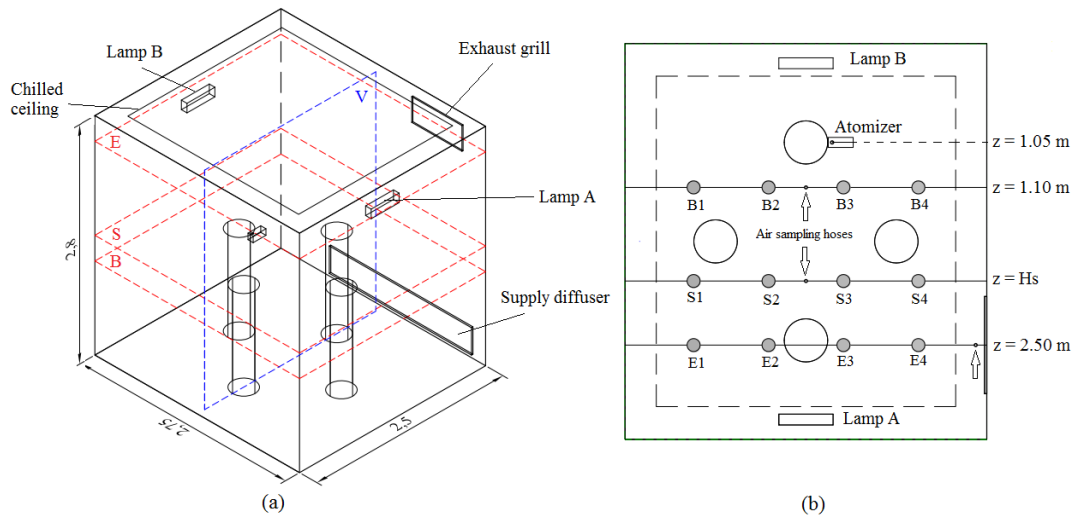


Fig. 5: Schematics of the *CC/DV* room (a) isometric view showing the vertical sampling plane (V) and horizontal planes (B, S, and E), and (b) top view showing the locations of the air sampling hoses. *H_s* denotes the stratification height.

C. Air Flow Measurements

An anemometer system (TSI, Model IFA 300 16 channels, accuracy 0.15%) equipped with a xyz traverse table is used to mount the probes in order to measure air velocity at different points.

In the horizontal air localization room the velocity and turbulence measurements are taken at the outlet of one of the four identical supply slots using uni-directional hot-wire anemometers manufactured by TSI (model IFA-300).

The anemometers have a sensing head of diameter 3 mm and are calibrated for low velocity range measurements (< 2 m/s) using a wind tunnel. The calibration wind tunnel consists of an open tunnel, a fan to deliver the air with desired velocity range, a nozzle to shape the velocity profile, and a mesh arrangement to uniform and reduce the flow turbulence. The air speed was measured by both a hot wire anemometer and a pitot-static tube which does not require calibration and can be used as a reference for the hot wires.

Four hotwires are placed on a horizontal rod directly at the outlet of the rectangular supply slot (with ± 1 mm positioning accuracy) and the rod is manually moved in one direction from the center of the slot to its end. The obtained readings of air velocity and turbulence intensity are then averaged and used as inputs to the *CFD* model to define the boundary conditions at the supply slots. For validation purposes, the slot angled diffuser jet velocities are also measured at nine different locations on the center cross plane of the slot. Velocity and turbulence measurements are also made at the outlet of DV supply grill in the CC/DV room.

D. Thermal Measurements

Temperature is measured using calibrated type T thermocouples (± 0.3 °C) linked to the anemometer system. The temperature measurements are taken at steady state, which is assumed to be reached when the monitored temperatures reach nearly constant values with variation within ± 0.3 °C. The supply air temperature and the inner surface temperatures of the walls are measured in the two climatic rooms and used as boundary conditions in the simulations.

Since the study focused on the air quality while maintaining acceptable comfort conditions, it is important to validate the thermal flow field around the thermal cylindrical manikin by taking temperature measurements. A set of 9 T-type thermocouples with $\pm 0.3^\circ\text{C}$ accuracy are distributed around the cylinder in the horizontal air localization room as shown in Fig. 3.b to monitor the variations in the temperature field. All the thermocouples are at 1.5 cm apart from the cylinder surface, and connected to an OMEGA DaqPro data logger. In the vertical air localization room, ten thermocouples are mounted on wooden column to measure the vertical distribution of room temperature. Other ten thermocouples are mounted on the chilled ceiling plate and the average of the readings is also used as boundary condition in the simulation.

E. UV Field Measurements

The *UV* devices should be installed at a height of no less than 2.13 m for safety reasons (American Conference of Governmental Industrial Hygienists, 1999). The *UV* model of Wu et al. (2011) used in the simulations will be validated by actinometrical measurements made at different locations in the room. Actinometrical cells are installed in 16 locations as shown in Fig. 4c to measure the irradiation intensity in the occupied zone (locations 1, 7, 13 at 1 m) and in the upper *UV* zone (locations 9, 14, 16 at 2 m; 6, 8, 11 at 2.15 m; locations 3, 5, 12, 15 at 2.2 m; 2, 4, 10 at 2.4m).

The actinometrical cells are filled with a solution prepared by adding 1 g of potassium iodide to 10 ml of the prepared solution of 0.6 M iodide and 0.1 M iodate in 0.01 M borate (Rahn et al., 1999). This solution is optically opaque at 254 nm and is insensitive to room light. The *UV* irradiance is calculated using the measured *UV* absorbance of the actinometrical solution.

F. Measurements of airborne bacteria concentration and bacteria settling

Four experiments are performed at steady-state conditions at two different *DV* supply flow rates with and without the use of *UVGI*. The experimental conditions are summarized in Table 2. Before starting each experiment, the room should be flushed using HEPA-filtered ventilation air for 3 hours without recirculating any return air. Some experiments were repeated twice to ensure repeatability of the measurements. The error in concentration measurements and *CFU* counts for any repeated experiment was less than 9%.

Table 2: Experimental scenarios

Experiment number	Supply air flow rate (kg/s)	Supply air temperature (°C)	Chilled ceiling temperature (°C)	Operating UV lamps
I	0.11	20.2	18.3	None
II	0.11	20.4	18.1	A and B
III	0.22	21.4	19.5	None
IV	0.22	21.5	19.6	A and B

The performance of the *UVGI* system is tested using *S. marcescens* supplied by the Department of Pathology at the American University of Beirut Medical Center (AUBMC). A suspension of *S. marcescens* (10^8 CFU/mL) is introduced using a six-jet atomizer (Model 9306A, TSI, Inc., USA) which generates droplets smaller than 10 μ m. The atomizer is located inside the room to avoid the use of long supply hoses where significant deposition of suspension droplets might occur (Fig. 5). The atomized bacteria suspension is released near the top of a heated cylinder 1.05 m above the floor at flow rate 12 L/min and pressure 138KPa. In order to maintain a constant atomization rate without the need for replenishment during the experiment, the atomizer is filled

with a relatively large amount of 350 mL of bacteria suspension. A set of measurements of suspension discharge from the atomizer throughout the experiment duration indicated this amount of bacteria is sufficient. The volumetric flow rate of the suspension leaving the atomizer is about 0.25 mL/min.

The indoor *S. marcescens* concentration is measured using the air sampling method. This method consists to extract a significant volume of air into a sterile solution that will be analyzed to determine the viable bacteria count per unit of air volume. Sampler inlets are placed at three different heights inside the room labeled as follows (Fig. 5b): the breathing level of a seated adult 1.1 m from the floor (label: B), stratification height (label: S), and room exhaust (label: E). In each experiment, the bacteria generation is started and maintained for 120 minutes, and during the last 30 minutes of generation air samples are collected.

Air samples are collected using constant flow air sampling pumps (SENSIDYNE, Gilian 5000, USA) at 2.75 ± 0.1 L/min through glass impingers (ACE GLASS, 25mL) each containing 10 mL of phosphate-buffered saline (PBS) that is autoclaved under a temperature 115°C for 15 minutes (Fig. 6).

The impinged liquids are placed onto agar plates that had been incubated at 35°C for 36 hours. The concentration of culturable airborne bacteria (CFU/L) is calculated as:

$$C = \frac{NV}{QT_{ext}} \quad (13)$$

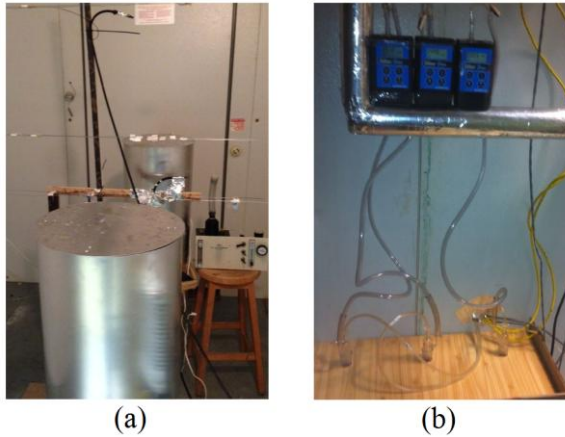


Fig. 6: Pictures showing the (a) heated cylinders, air sampling hoses, atomizer, and (b) air sampling hoses connected to impingers

where N is the average number of CFU per liter of the sterile solution (CFU/L), V is the final impinger volume (L), Q is the sampling air flow rate (L/min), and T_{ext} is the total sampling time (min).

In order to measure the bacteria deposition, settle petri plates of standard diameter of 90 mm with a convenient agar-based growth medium are used in the experimental facility. Four plates are evenly distributed and exposed at each of the three aforementioned heights (breathing level, stratification level, and exhaust level) and labeled accordingly as shown in Fig. 5b.

The plates are initially covered at the beginning of each experiment, and then uncovered after two hours and kept exposed for another two-hour period of time. After incubation, the count of *S. marcescens* colony forming units on each plate is reported to indicate the number of viable bacteria that deposited on each plate.

CHAPTER VII

SIMPLIFIED MODELING OF PATHOGEN TRANSPORT

UVGI SPACES CONDITIONED WITH CC/DV

The stratified *DV* air flow makes plume multi-layer models of *CC/DV* conditioned spaces take a physical approach to the problem where the space may be divided into horizontal air layers. Given that these simplified models are computationally less expensive than 3D CFD models, the multi-layer model of Kanaan et al. (2010) for contaminant transport in *CC/DV* systems and the analytical three-zone model of Noakes et al.(2004) for *UR-UVGI* systems are integrated in this work. The integrated model is meant to serve as a simple predictive tool for the bacteria vertical distribution in *CC/DV* rooms with and without upper room UV field.

A. Plume Multi-zone Multi-layer Model for Airborne Transport of Pathogens

In displacement ventilation, the cooler air entering the room at the floor level displaces the warmer room air that rises due to its natural buoyancy effect. Consequently, the bottom occupied zone contains the fresh cool air with no recirculation flow while the heat and contaminants produced by the room activities rise to the ceiling level where they are exhausted. The driving force of the plume is the temperature difference between the plume and the surroundings. When this difference diminishes, the plume reaches its terminal height at which it spreads horizontally to

delimit an upper mixing zone. Two zones with opposite unidirectional flows are identified below the plume terminal height in the surroundings of the plume. The interface between the two zones is called the stratification height and is defined as the level where the air flow rates of plume and wall plumes are balanced with the supply air flow rate. The radiation heat transfer exchange is considered between the occupants and surfaces around them including the inner faces of the walls, and the chilled ceiling. The direct and reflected long wave radiation elements are included as in Keblawi et al. (2011). The chilled ceiling then carries part of the sensible load by direct radiation and convection. The number of 10 layers produces grid independent results and the error in numerical results is less than 2% when compared to those obtained for twelve and fourteen layers. The mass flow in and out of each layer due to heat sources is calculated from the plume equations reported by Mundt (1996). The room is conceptually divided into the following seven air zones (see Fig. 7):

- Zone I: single-layer floor zone where the air is supplied;
- Zone II: multi-layer stratification zone bounded by the stratification height (H_s) and floor zone;
- Zone III: wall plume zone associated with wall buoyant flow
- Zone IV: multi-layer plume zone from plume virtual source height to the terminal height;
- Zone V: multi-layer air zone outside the plume bounded by H_s and terminal plume height z_t ;
- Zone VI: single-layer lower mixed-air zone between z_t and z_{UV} ; and
- Zone VII: single-layer upper mixed-air UV -zone in which air is irradiated.

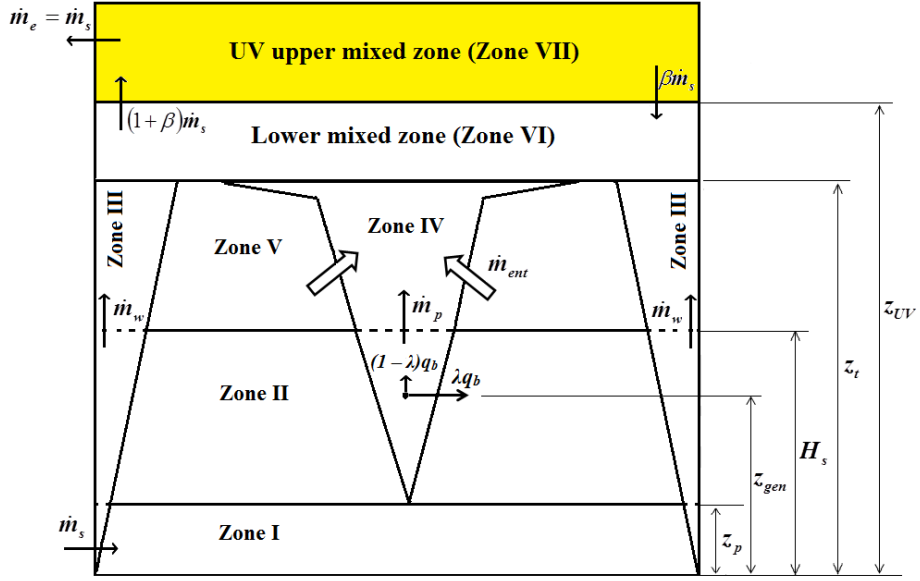


Fig. 7: Schematic of the zonal distribution of DV room equipped with UVGI.

The interface heights that delimit the zones are the stratification height H_s , plume terminal height z_t , and UV zone height Z_{UV} . z_t is the elevation at which the density gradients disappear in the rising air and the plume spreads horizontally, and z_{UV} is the height above which UV -Irradiation is significant. The plume terminal height (z_t) is given by Mundt (1996) as follows:

$$z_t = 0.74\Phi^{1/4}(dT/dz)^{-3/8} \quad (14)$$

Where Φ is the source convective heat flux, T is the environment temperature, and z is the vertical coordinate. The stratification height is considered in general as an indicator of good air quality if it is higher than 1.2 m (height of a seated person) where it determines the height of the occupied zone below which air air CO_2 concentration should not exceed 700 ppm (Kanaan et al., 2010). The upper-room $UVGI$ irradiates air in the upper-mixed zone at uniform UV irradiance, E (W/m^2) but does not cover the entire fully-mixed region above the plume terminal height. The lower mixed zone is assumed to have less significant UV field especially when louvered UV lamps are used.

The transport equations of bacteria depend on zonal mass and momentum transport of air. Air is supplied at flow rate (\dot{m}_s) at the floor level and moves upward (see Fig. 7). A heat source of power Φ at height z_p generates an upward plume flow (\dot{m}_p) induced by buoyancy and entrains air flow (\dot{m}_{ent}) from adjacent air zones. In addition, the warm wall induces a wall plume (\dot{m}_w) by entrainment of adjacent room air. Bacteria and CO₂ are generated from occupants at rates q_b and q_c , respectively assuming the breathing mode. The room air moves up until it reaches the stratification height H_s above which it recirculates since plume flow rate in that zone exceed supply flow rate. The zone below the terminal height exchanges recirculation air from the lower-mixing zone. Moreover, inter-zonal air mass flow rate exchanges take place between lower mixed zone and upper UV -zone. The plume flow rates and inter-zonal mass flow rates that will be used in the multi-layer model will be defined in this section. The downdraughts from the chilled ceiling are neglected.

The plume average upward mass flow rate \dot{m}_p is calculated using Mundt (1996) correlation as a function of height from the heat source at power Φ and vertical temperature gradient dT/dz of room air as follows:

$$\dot{m}_p = 0.00238\Phi^{3/4} (dT/dz)^{-5/8} B_1 \quad (15a)$$

$$B_1 = 0.004 + 0.039A_1 + 0.38A_1^2 - 0.062A_1^3 \quad \text{and} \quad A_1 = 2.86z(dT/dz)^{3/8} \Phi^{-1/4} \quad (15b)$$

The mass flow rates of wall plumes (\dot{m}_w) are given by Jaluria (1980) as:

$$\dot{m}_w = 2.87 \times 10^{-3} \rho (\Delta T_w)^{1/4} z^{3/4} Y \quad (16)$$

where Y is the wall width and ΔT_w is the wall-air temperature difference. Since our heat source is assumed cylindrical of diameter d and height H_c , it is replaced by a virtual

point source such that the border of the plume above the point source passes through the upper edge of the real cylindrical source. The position of the virtual source will be located at $z_0 = 1.8 d$ below the actual source (Goodfellow, 2001). The virtual source will then be located at $z_p = H_c - z_0$ and the vertical distance to be used in the plume flow rate equations (15a and 15b) is $(z - z_p)$. The flow rate resulting from a warm wall (\dot{m}_w) is determined from Ayoub et al. (2006) multilayer wall-plume model correlations. Even though not all heat sources are bacteria emitting sources, multiple heat sources are lumped into one source of an equivalent heat output and contaminant generation. This approximation would be reasonable since the stratification height is governed by resultant plume flow which is the sum of all single plume flow rates.

The inter-zonal exchanges in the upper region are important for determining bacteria inactivation and their modeling would follow the mixed two-zone model of Noakes et al. (2004). The inter-zonal air flow rate (\dot{m}_{ex}) relative to the absolute room supply flow rate (\dot{m}_s) was defined by Noakes et al. (2004) as follows:

$$\beta = \frac{\dot{m}_{ex}}{\dot{m}_s} \quad (17)$$

where β is a dimensionless mixing factor. The inter-zonal flow rate \dot{m}_{ex} is given by

$$\dot{m}_{ex} = \frac{\rho A U_{int}}{2} \quad (18)$$

where A is the interface area and U_{int} is the inter-zonal velocity which can be determined from the layer mass balance.

To develop the airborne bacteria transport equations, we will follow the model of Ayoub et al. (2006) for heat transport in CC/DV conditioned spaces and the multi-layer model of Kanaan et al. (2010) for contaminant transport for zones below the

terminal height. The multilayer plume model solves the mass and energy balances for air flow and determines the room stratification height and thermal gradient for given supply flow rate, supply temperature and chilled ceiling temperature. The energy balances will not be derived here and can be found in the work of Ayoub et al. (2006). The room supply conditions are determined such that the stratification height is above 1.2 m and temperature gradient does not exceed 2.5 °C/m (Ghaddar et al., 2008; Mossolly et al., 2008).

Fig. 8 shows a schematic of the air and plume layers in the space selected for our analysis. The room is divided to 10 layers. The first layer extends from $z = 0$ at the floor level up to the thermal plume virtual source height z_p . The breathing region is considered to span layers 4 and 5. The bacteria and CO₂ are generated at constant rates in layer 4 that is assigned a small grid height to avoid high concentration gradient at this level and ensure accuracy. Layers 6-8 are equal in height and represent the region between the stratification height and terminal plume height. Layers 9 and 10 represent the two lower and upper zones of the fully-mixed zone previously defined. It is also assumed that the plume terminal height is always below the fully mixed zone.

The mathematical model for airborne bacteria transport is presented here based on mass balances for each layer in the different zones and it will predict the bacterial concentration C (CFU/m³) in room air and inside plumes, in a typical CC/DV room with the presence of an upper room UV field at uniform-intensity E .

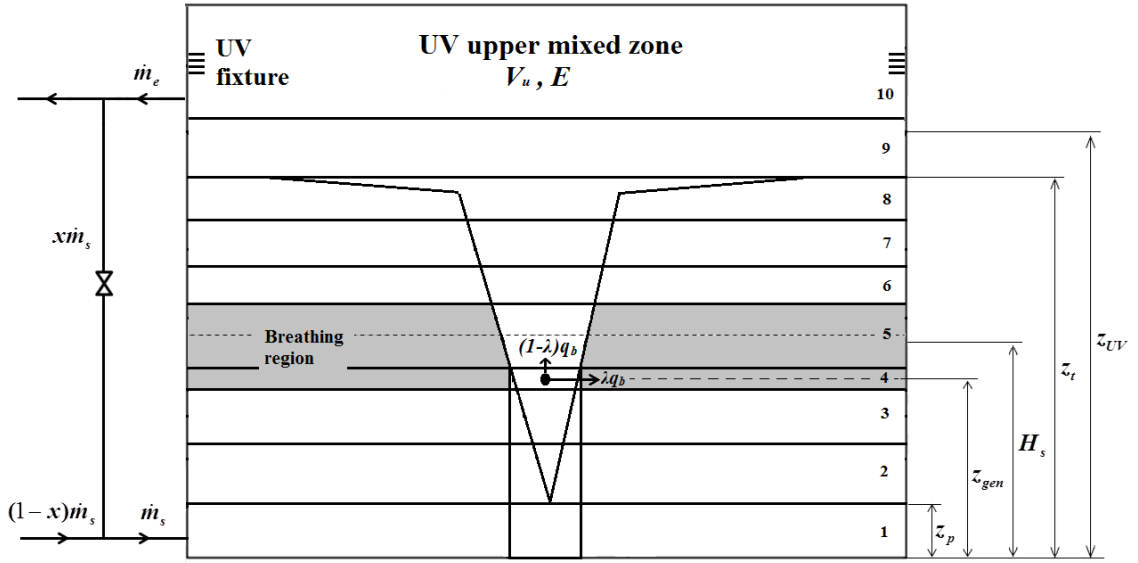


Fig. 8: Schematic of mathematical model with upper UV field.

The net circulated flow rate \dot{m}_{cir} at each height z representing the layer height is calculated as

$$\dot{m}_{cir} = \dot{m}_s - \sum_{i=1}^n \dot{m}_{p,i} - \sum_{j=1}^h \dot{m}_{w,j} \quad (19)$$

where n is the number of heat sources and h is the number of hot walls. Assuming control volumes with only one-dimensional inlets and outlets, the steady-state mass balance for Layer 1 is given by

$$\dot{m}_s C_s + A_1 D \rho \left(\frac{\partial C}{\partial z} \right)_1 = \dot{m}_s C_1 \quad (20)$$

In the above equation, C_s is the airborne bacterial concentration in the supply air stream. The second term on the left side of Eq. 20 is diffusion through the interface of area A_1 with Layer 2, D is the molecular diffusion coefficient of bacteria, and C_1 is the room air bacterial concentration of Layer 1. The gravitational settling and deposition of bacteria on walls and surfaces are not accounted for in the model due to the very small size of

bacteria carriers (< 5 microns).

Diffusion from wall plumes to the room air is neglected since wall plumes are not emitting sources and the difference in contaminant concentration between room air and the wall plume is too slight.

The bacteria mass balance for the air layer k ($k = 2$ to 8) is given by

$$\begin{aligned} \left(\dot{m}_{cir,k-1} + \sum_{j=1}^h \dot{m}_{w,j,k-1} \right) C_{k-1} - A_{int,k} (D + D_t) \rho \left(\frac{\partial C_p}{\partial r} \right)_{z_{m_k}} + A_k D \rho \left(\frac{\partial C}{\partial z} \right)_{z_{m_k}, z_{m_{k+1}}} + \lambda \rho q_k \\ = \left(\dot{m}_{cir,k} + \sum_{j=1}^h \dot{m}_{w,j,k} \right) C_k + \dot{m}_{ent,k} C_k + A_{k-1} D \rho \left(\frac{\partial C}{\partial z} \right)_{z_{m_{k-1}}, z_{m_k}} \end{aligned} \quad (21)$$

The first term in the left side of Eq. 21 is the convective term associated with air transport and the second term is the diffusion between the plume and adjacent air layer at the middle of that layer. The bacterial concentration inside the plume is C_p , r is the radial coordinate from the plume centerline, \dot{m}_{ent} is the mass entrained by the plume from the adjacent air layer. The molecular diffusion coefficient D is augmented by adding turbulent diffusion coefficient D_t due to the turbulent nature of the plume at its boundaries. This coefficient was correlated to plume upward velocity and characteristic turbulent length that is the plume width at any height (Chen and Xu, 1998). The parameter λ is the fraction of exhaled bacteria that traverse the plume and reach the adjacent room air and q_k is the volumetric bacteria flow rate generated in layer k . In the current case of exhaled jet of low velocity, λ can be reasonably assumed zero since the exhaled air is pulled up by the rising thermal plume (Russo and Khalifa, 2011). In cases of exhaled airflow of high momentum, the most suitable value of λ should be identified using *CFD* models and comparing results with simplified model at different values of λ to obtain the best fit value.

The bacteria mass balance inside the plume in layer k ($k=2$ to 8) is given by:

$$\begin{aligned} \dot{m}_{p,k-1}C_{p,k-1} + \dot{m}_{ent,k}C_k + (1-\lambda)\rho q_k + A_{p,k-1}D\rho\left(\frac{\partial C_p}{\partial z}\right)_{z_{m_{k-1}},z_{m_k}} = \\ \lambda\rho q_k - A_{int,k}(D+D_t)\rho\left(\frac{\partial C_p}{\partial r}\right)_{z_{m_k}} + A_{p,k}D\rho\left(\frac{\partial C_p}{\partial z}\right)_{z_{m_k}-z_{m_{k+1}}} + \dot{m}_{p,k}C_{p,k} \end{aligned} \quad (22)$$

where \dot{m}_p is the mass flow rate of the plume at the boundary, A_p is the plume area at the interface, and q_k is the volumetric bacteria flow rate generated in layer k where q_k is q for $k = 4$ and zero otherwise.

The bacteria mass balance in Layer 9 which is the lower mixing zone of the fully-mixed region described previously is given by the following equation where β is the mixing factor defined in Eq. 17:

$$\left(\sum_{j=1}^h \dot{m}_{w,j,8}\right)C_8 + \beta\dot{m}_sC_{10} + A_{p,8}D\rho\left(\frac{\partial C_p}{\partial z}\right)_{z_{m_8},z_{m_9}} = (1+\beta)\dot{m}_sC_9 + A_8D\rho\left(\frac{\partial C}{\partial z}\right)_{z_{m_8},z_{m_9}} + \dot{m}_{cir,9}C_9 \quad (23)$$

The bacteria mass balance in the *UV* upper zone (Layer 10) is given by

$$(1+\beta)\dot{m}_sC_9 = \beta\dot{m}_sC_{10} + \dot{m}_eC_{10} + \rho ZEV_uC_{10} \quad (24)$$

The term ZEV_u is the *UV* bacteria inactivation constant where V_u is the volume of the *UV* upper zone and Z is the bacteria susceptibility to *UV*.

Ignoring bacteria deposition in return duct and assuming zero concentration of pathogens in the fresh air, the bacterial concentration in the supply air when mixed with return air can then be calculated as:

$$C_s = xC_{10} \quad (25)$$

where x is the return mixing ratio.

The linear bacteria transport equations (20) to (25) are discretized using finite difference method. They are solved to find the unknowns: C_2 to C_{10} and C_{p2} to C_{p8} . The details of the numerical solution methodology used to solve the obtained system of equations were presented in (Kanaan et al., 2010). The developed model accounted for the convection through layers, the diffusion between layers, plumes and room air and it

will be validated by detailed *CFD* simulations. The indoor air quality is assessed based on the bacterial concentration of the room air averaged in the breathing zone for layers 4 and 5 as shown in Fig. 8 and should meet the WHO standard of not to exceed 500 CFU/m³ (WHO, 1988).

B. Extended Plume Multi-zone Multi-layer Model for Pathogen Transport at Different Particle Sizes

In order to provide accurate predictions of airborne pathogen concentration, the model should account for the principal physics that affect the particle/bacteria behavior such as convection, molecular and turbulent diffusion, deposition, and gravitational settling. Saliva droplets that are larger than 20 μm rapidly settle onto surfaces (Gold and Nankervis, 1989), while droplets between 0.5 and 20 μm remain in the air for long periods and are more likely to be captured in the respiratory tract and produce infection (McCluskey et al., 1996). For pathogen-carrying droplets smaller than 20 μm , the deposition effect may be neglected as droplets in this size range evaporate quickly and remain in the air for long periods of time. However, the inclusion of gravitational settling and deposition is necessary when modeling larger particles that may settle rapidly onto surfaces. It is assumed that all the surfaces in the modeled space are either horizontal or vertical. The deposition velocities including the Brownian and turbulent diffusion in addition to the gravitational settling effect on particle behavior for vertical walls, floor, and ceiling are given respectively by the following expressions (Lai and Nazaroff, 2000):

$$v_{d,w} = \frac{u^*}{I} \tag{26a}$$

$$v_{d,f} = \frac{v_s}{1 - \exp\left(\frac{-v_s I}{u^*}\right)} \quad (26b)$$

$$v_{d,c} = \frac{v_s}{\exp\left(\frac{v_s I}{u^*}\right) - 1} \quad (26c)$$

where v_s is the settling velocity calculated using the saliva droplet density and size, and air dynamic viscosity as follows:

$$v_s = \frac{\rho_d p^2 g}{18\mu} \quad (26d)$$

I is an integral number given by:

$$I = 3.64Sc^{2/3}(a-b) + 39 \quad (26e)$$

$$a = \frac{1}{2} \ln \left[\frac{(10.92Sc^{-1/3} + 4.3)^3}{Sc^{-1} + 0.0609} \right] + \sqrt{3} \arctan \left[\frac{8.6 - 10.92Sc^{-1/3}}{10.92\sqrt{3}Sc^{-1/3}} \right] \quad (26f)$$

$$b = \frac{1}{2} \ln \left[\frac{10.92Sc^{-1/3} + r^+)^3}{Sc^{-1} + 7.669e^{-4}(r^+)^3} \right] + \sqrt{3} \arctan \left[\frac{2r^+ - 10.92Sc^{-1/3}}{10.92\sqrt{3}Sc^{-1/3}} \right]$$

u^* is the friction velocity with a typical value of 1.5 cm/s in indoor environments

After including gravitational settling and deposition of the pathogen-carrying particles, the steady-state airborne bacteria mass balance for Layer 1 adjacent to the floor is given by:

$$\dot{m}_s C_s + A_1 \rho v_s C_2 + A_1 \rho D \left(\frac{\partial C}{\partial z} \right)_1 = \left(\dot{m}_s + \rho v_{d,f} A_f + \sum_{j=1}^h \rho v_{d,w,j} A_{w,j,1} \right) C_1 \quad (27)$$

In the above equation, v_s is the settling velocity of the bacteria-carrying particle, and $v_{d,f}$ and $v_{d,w,l}$ are the particle deposition velocities on the floor and the walls within Layer 1 respectively.

The bacteria mass balance for the air layer k ($k = 2$ to 8) is given by:

$$\begin{aligned} & \left(\dot{m}_{cir,k-1} + \sum_{j=1}^h \dot{m}_{w,j,k-1} \right) C_{k-1} - A_{int,k} (D + D_t) \rho \left(\frac{\partial C_p}{\partial r} \right)_{z_{m_k}} + A_k \rho v_s C_{k+1} + A_k \rho D \left(\frac{\partial C}{\partial z} \right)_{z_{m_k}, z_{m_{k+1}}} \\ & = \left(\dot{m}_{cir,k} + \dot{m}_{ent,k} + A_{k-1} \rho v_s + \sum_{j=1}^h \dot{m}_{w,j,k} + \sum_{j=1}^h \rho v_{d,w,k} A_{w,j,k} \right) C_k + A_{k-1} \rho D \left(\frac{\partial C}{\partial z} \right)_{z_{m_{k-1}}, z_{m_k}} \end{aligned} \quad (28)$$

The bacteria mass balance inside the plume in layer k ($k=2$ to 8) is given by:

$$\begin{aligned} & \dot{m}_{p,k-1} C_{p,k-1} + \dot{m}_{ent,k} C_k + \rho q_k + A_{p,k} \rho v_s C_{p,k+1} + A_{p,k-1} D \rho \left(\frac{\partial C_p}{\partial z} \right)_{z_{m_{k-1}}, z_{m_k}} = \\ & A_{p,k-1} \rho v_s C_{p,k} - A_{int,k} (D + D_t) \rho \left(\frac{\partial C_p}{\partial r} \right)_{z_{m_k}} + A_{p,k} D \rho \left(\frac{\partial C_p}{\partial z} \right)_{z_{m_k}, z_{m_{k+1}}} + \dot{m}_{p,k} C_{p,k} \end{aligned} \quad (29)$$

The bacteria mass balance in Layer 9 which is the lower mixing zone of the fully-mixed region described previously is given by the following equation:

$$\begin{aligned} & \left(\sum_{j=1}^h \dot{m}_{w,j,8} \right) C_8 + \beta \dot{m}_s C_{10} + A_9 \rho v_s C_{10} + A_{p,8} D \rho \left(\frac{\partial C_p}{\partial z} \right)_{z_{m_8}, z_{m_9}} = \\ & \left[(1 + \beta) \dot{m}_s + \dot{m}_{cir,9} + A_8 \rho v_s + \sum_{j=1}^h \rho v_{d,w,9} A_{w,j,9} \right] C_9 + A_8 D \rho \left(\frac{\partial C}{\partial z} \right)_{z_{m_8}, z_{m_9}} \end{aligned} \quad (30)$$

The bacteria mass balance in the *UV* upper zone (Layer 10) is then given by

$$(1 + \beta) \dot{m}_s C_9 = \left(\beta \dot{m}_s + \dot{m}_e + A_9 \rho v_s + A_c \rho v_{d,c} + \sum_{j=1}^h \rho v_{d,10} A_{w,j,10} + \rho ZEV_u \right) C_{10} \quad (31)$$

The predictions of the extended simplified model for bacteria concentrations are compared with experimental results for droplet size less than $10 \mu\text{m}$ (from the atomizer) with average equilibrium diameter of droplet nuclei $2.5 \mu\text{m}$. The room is simulated with and without upper room *UVGI* using both *CFD* and mathematical model for all the experimental scenarios.

Chapter VIII

Results and Discussion

A. Horizontal Air Localization System

1. *Experimental Validation of the CFD Model*

According to Chen and Srebric (2000), validating the flow and thermal properties obtained at the boundaries (diffuser outlets) is the most important for accurate predictions in ventilation problems. Flow and thermal parameters near boundaries and at inlets have the highest spatial gradients. For that reason, the velocities at the outlets of the angled diffuser are experimentally obtained. Furthermore, near body field temperature is also measured and compared to *CFD* predictions.

The experimentally measured air velocities at different positions away from the supply slot are used to validate the simulated jet. For these velocity measurements, air is supplied from the diffuser at flow rate $0.056 \text{ m}^3/\text{s}$ and temperature 16.2°C . The average of recorded air velocities along the supply slot is 1.93 m/s and average experimental value of 0.14 is obtained for turbulence intensity. Fig. 9 shows good agreement between the *CFD* predictions and measurements of jet velocities at 8 different points labeled on the jet profile diagram. The maximal relative error between predicted and measured values of the velocity is 8% showing that the diffuser geometry is reasonably simulated.

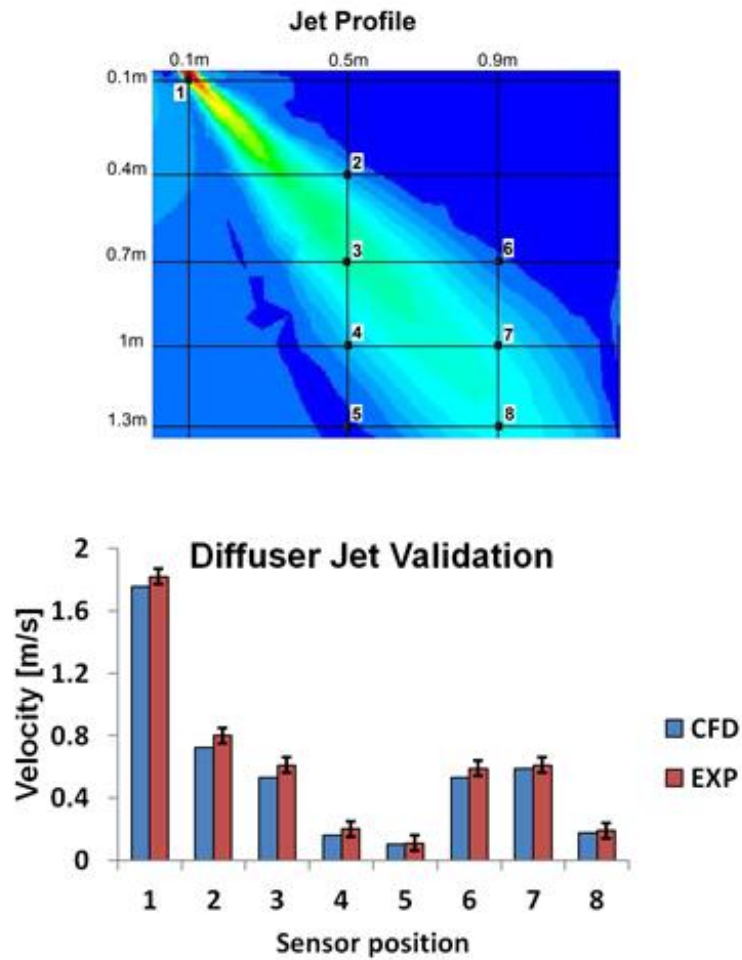
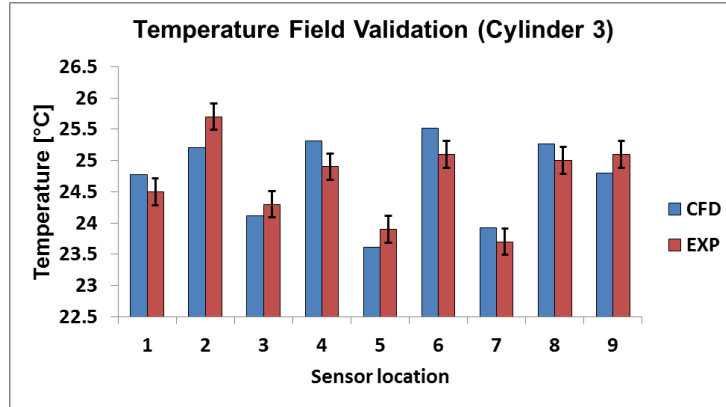
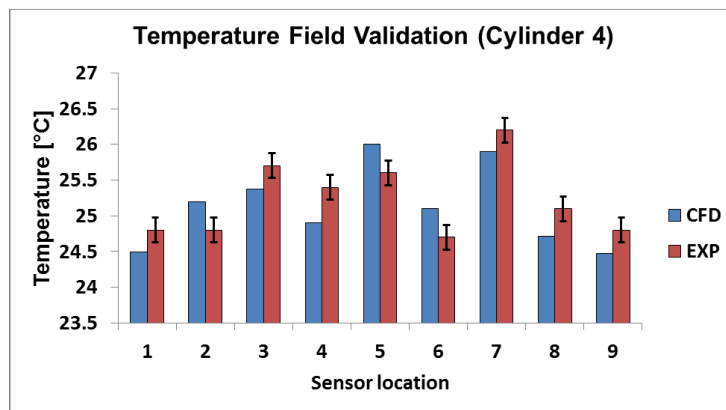


Fig. 9: Plot of the measurements and CFD predictions of air velocity at 8 labeled positions on the jet profile diagram.

The measured inner surface temperatures of the vertical walls are 25.2 °C, 24.9 °C, 25.1 °C, 25.4 °C and are used in the simulation as wall boundary conditions. Fig. 10 shows that the CFD predictions and experimental data of temperatures in the vicinity of cylinders 3 and 4 compare well with a maximal relative error of 5%.



(a)



(b)

Fig. 10: Plot of the predicted and measured temperatures in the vicinity of (A) cylinder 3 and (B) cylinder 4.

Table 3 shows the *UV* irradiance intensities computed from the model of Wu et al. (2011) and those measured using actinometrical cells. The radiation intensity measurements compared well with the model values with a relative error of 10-15%.

Table 3: Distribution of UV irradiance in W/m^2 inside the horizontal air localization room

Operating lamps	Average intensity in the upper zone		Average intensity in the occupied zone (model)	Intensity range in the occupied zone (measurements)
	Model	Measurements		
A	0.2128	0.2498	0.0199	0.012 - 0.021
B & C	0.3039	0.3567	0.0315	0.029 - 0.044
A, B & C	0.4267	0.4777	0.0528	0.051 - 0.069

The flow, thermal, and bacteria concentration fields obtained from *CFD* simulations at a midplane in the experimental room are shown in Fig. 11. Curtain jets are formed delimiting the localized zone around the cylinders within the conditioned space, and provide the desired thermal containment.

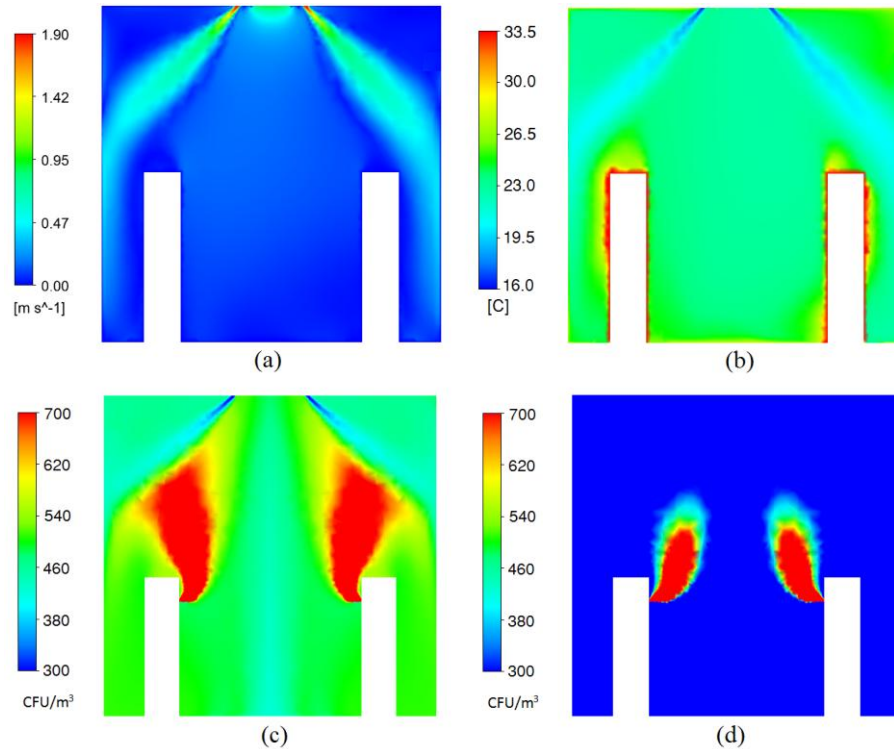


Fig. 11: Plots of (A) the velocity distribution in the room, (B) air temperature distribution, (C) *S. marcescens* distribution when UVGI is OFF and (D) *S. marcescens* distribution when the three un-louvered 18 W UV lamps are operated.

Moreover, the air velocity and temperature are averaged in the occupant microclimates for thermal comfort assessment. The microclimate of each of heated cylinders 3 and 4 is defined as a rectangular zone surrounding the cylinder at a distance of 30 cm from its sides and top. The average air velocity in the microclimate of cylinder 3 is 0.12 m/s and 0.10 m/s in that of cylinder 4, while the mean air temperature is 23.7 °C and 24.3 °C respectively. This, according to *ASHRAE* standard 55-2013, results in a percentage of people dissatisfied people (PPD) less than 6%, which confirms

that thermal comfort is reasonably achieved. The distribution of *S. marcescens* in the modeled space for a supply air concentration of 300 CFU/m^3 without the use of *UVGI* is shown at the symmetry plane in Fig. 11 (c-d) for the case without the use of UV lamps and when the three un-louvered 18 W germicidal lamps are operated, respectively. The predicted disinfection rate achieved based on the steady-state bacteria concentration at the room exhaust is 85.2%.

Fig. 12 displays the containment effect of the localizing airflow that results in minimal air mixing between the two adjacent environmental zones.

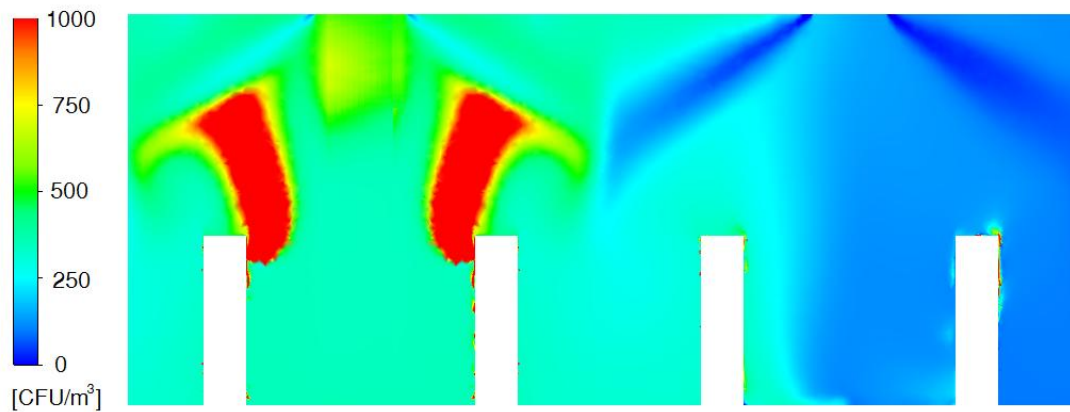


Fig. 12: Plot of bacteria concentration of in the large space with two ceiling localized system when bacteria is emitted in one zone.

The IAQ in each zone is assessed based on the predicted bacteria concentration in the breathing layer. The breathing layer is defined in the CFD domain as being the horizontal air layer between $z = 0.88 \text{ m}$ and $z = 1.22 \text{ m}$.

Although a return air fraction of 30% is used, the predicted volume-average bacteria concentration in the breathing layer of the zone with no bacteria generation (the right-hand localized air zone) is acceptable of 324 CFU/m^3 ($< 500 \text{ CFU/m}^3$). On the other hand, a value of 623 CFU/m^3 is predicted for the zone with bacteria emission (the

left-hand localized zone). These values indicate that the localized air distribution system is effective in preventing cross-infection between the two adjacent zones.

2. Validation of the CFD-UV Model with Published Data

In order to validate the developed *CFD-UV* model, the bacteria concentration is predicted for the setup described in the published work of Miller and Macher (2010) in which they experimentally measured bacteria concentration and investigated the efficacy of germicidal lamps in reducing airborne bacteria. The scenarios concerned for validating our *CFD* model applied to Miller and Macher's room are those with a single unlouvered 15 W *UV* lamp and constant generation of three cuturable bacteria *B. subtilis*, *E.coli*, and *M. luteus*. The average *UV* irradiance at the breathing level and ceiling level are reported at 0.0069 W/m² and 0.25 W/m² respectively, whereas the values of 0.0084 W/m² and 0.19 W/m² are numerically obtained using our current radiation model. The concentrations of bacterial aerosol at the exhaust reported by Miller and Macher (2000) through counting of colony-forming units, with and without *UVGI*, are compared with current *CFD* model results to evaluate the effectiveness of *UVGI* model at steady-state conditions. The values of *UVGI* effectiveness using *M. luteus*, *B. subtilis*, and *E. coli* obtained from the *CFD* model are respectively 0.45, 0.53, and 0.99 that agreed reasonably with the experimental values of 0.49, 0.56, and 1 reported by Miller and Macher (2000) .

B. Vertical Air Localization (CC/DV) System

1. Experimental Validation of the CFD Model

Measured air temperatures and velocities of our current experiment are compared to values obtained from *CFD*. Table 4 shows a comparison between measured velocities and those obtained from *CFD* at points of specified coordinates relative to the origin of the room located in the far right corner of the room.

Table 4: Velocity measurements and values obtained from CFD

Point	Measured Velocity (m/s)	Velocity computed by <i>CFD</i> (m/s)
(109, 143, 70)	0.1367	0.1212
(109, 143, 84)	0.1326	0.1191
(109, 143, 90)	0.1985	0.1771
(109, 143, 103)	0.1663	0.1495
(109, 143, 114)	0.1567	0.1388
(141, 158, 77)	0.1238	0.1104
(141, 158, 55)	0.1386	0.1181
(140, 167, 55)	0.1053	0.0933
(140, 167, 65)	0.1223	0.1057
(140, 167, 100)	0.1118	0.0988

Measured and computed velocities show very good agreement with root-mean-square error of 0.016 m/s. The comparative plot shown in Fig. 13 shows that the temperature measurements and values obtained from *CFD* agree reasonably with a maximal relative error of 3%.

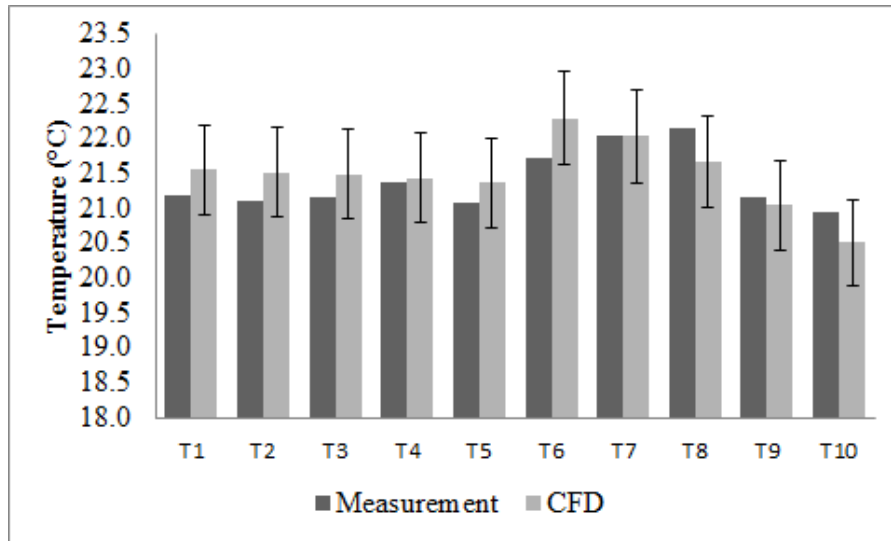


Fig. 13: Comparative plot of measured and CFD values of room air temperature distribution.

2. CFD Validation of the Airborne Bacteria Transport Plume Multi-layer Multi-zone Model (with no deposition)

The comparison of the predicted bacteria concentrations of the simplified model with those obtained from *CFD* are performed for a base case with same load as the experimental room with four occupants of which two are bacteria-emitting fresh *DV* supply air. To find an equivalent concentration value in CFU/m^3 (adopted unit in WHO standard, 1988), the molar fraction is multiplied by the density of bacteria-carrying droplets in kg/m^3 and then divided by the mass of one bacterium. The CFU conversion assumes that each colony forming unit arises from a single viable bacterium which is quite conservative in assessing the cleanliness of air. The *CFD* simulations produced the velocity, temperature, and CO_2 concentration fields as well as bacteria concentration field in molar fraction in the space.

Fig. 14 shows the room velocity vector field on the sampling plane V (Fig. 5). The airflow established in the room is almost upward in the lower zone and is recirculating in the upper zone. The level at which no circulation occurs is the stratification height is at 1.32 m which is sufficiently high to provide thermal comfort and acceptable air quality in the occupied zone.

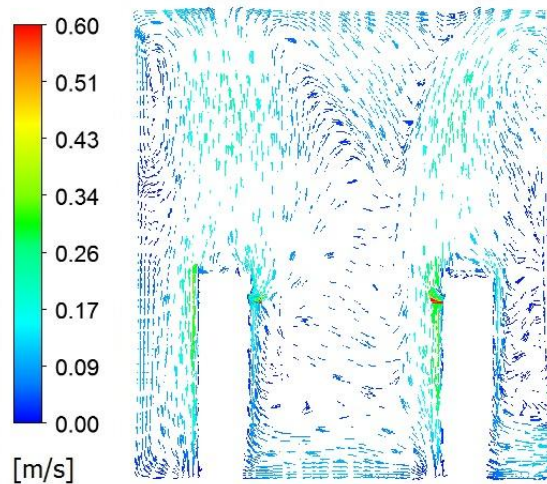


Fig. 14: Room velocity vector field.

Temperature and carbon dioxide concentration spatial distributions on the sampling plane are presented in Fig. 15 where two zones can be identified: lower cool and clean zone, and upper warm and contaminated separated by the stratification height. The cool air supplied to the room warms due to heat exchange with the heat source and moves upward by buoyancy entraining the contaminant to the upper levels of the room. The room temperature gradient in the room is computed to be about 1.45 °C/m satisfying the thermal comfort condition of a maximal temperature gradient of 2.5 °C/m.

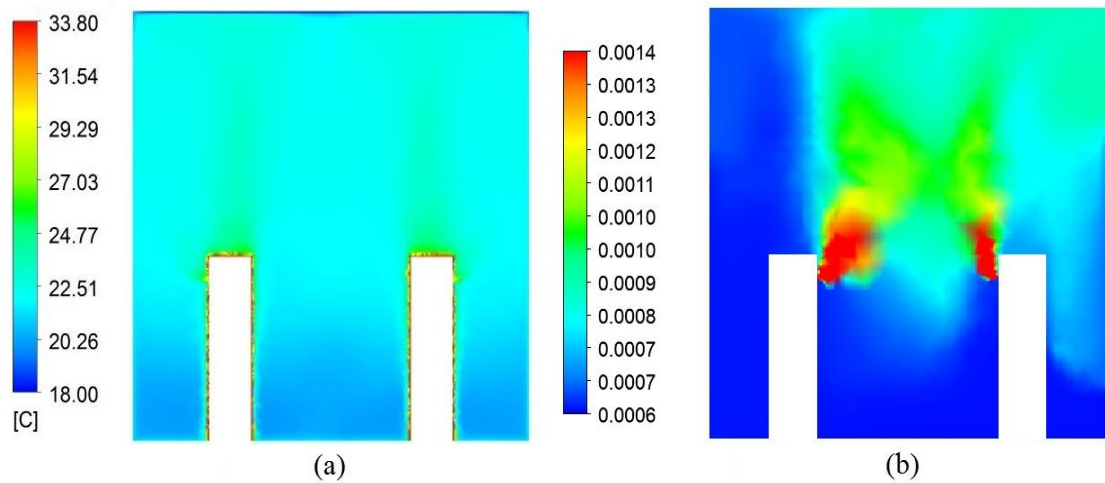


Fig. 15: (a) Thermal field and (b) CO₂ mass fraction distribution in the room.

S. aureus mass fraction distribution when UV device is OFF is shown in Fig. 16 on two horizontal cut planes at (a) height $z = 1.28$ m, (b) height $z = 2$ m. Fig. 16 shows also the bacteria distribution on the vertical sampling plane when (c) UV device is OFF and (d) UV device is ON . The pathogen is transported by the thermal plume around the heat source to the upper levels of the room leaving clean air in the occupied zone. The plots reveal the low diffusion of the bacteria that is much more concentrated in the plume where it is generated and mainly entrained by convection to the upper part of the room.

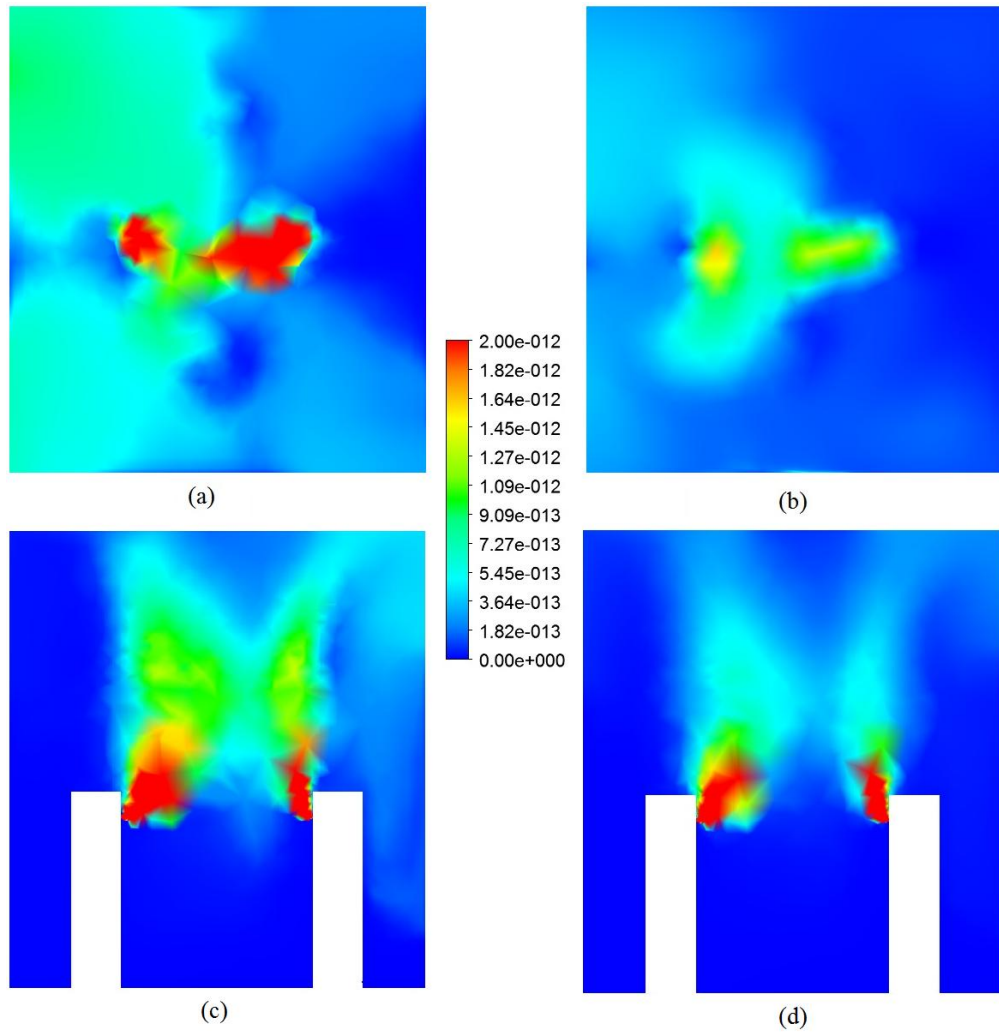


Fig. 16: Contour plots of bacteria mass fraction when UV lamps are OFF on horizontal cut planes at (a) $z = 1.28$ m, (b) $z = 2$ m, and on the sampling plane when UV lamps are (c) ON and (d) OFF.

The bacteria are not symmetrically distributed around the two sources despite their equal intensities because they are not symmetric with respect to the exhaust grill that extracts the flow surrounding the closer heat source.

When *UR-UVGI* system is operated, the bacterial concentration decreased significantly in the upper mixed zone and remains almost unchanged below stratification height.

The multi-layer model predicts the vertical bacteria concentration distribution for room air and in the plume as well as the mixing upper region including the UV zone.

Unlike CO₂ transport model of Kanaan et al. (2010) where all human sources are emitting sources, bacteria generation is not associated with all heating sources. It is important to ensure that treating all heat sources as single plume source in the bacteria transport model will still predict well the room air bacteria concentration.

The values of bacterial concentration obtained from the simplified model are evaluated as average values for each layer outside the plume from layer 1 to layer 10 and will be compared with bacterial concentrations predicted by the detailed 3-D CFD model averaged over each corresponding layer in the simplified model. The average bacteria concentration will be computed from the *CFD* model results for each layer volume. The height would represent the mid-layer coordinate z_m . Fig. 17 compares the multi-layer model and detailed CFD simulation predictions of bacteria concentrations as a function of height for room air (a) without use of UV and (b) while using UV.

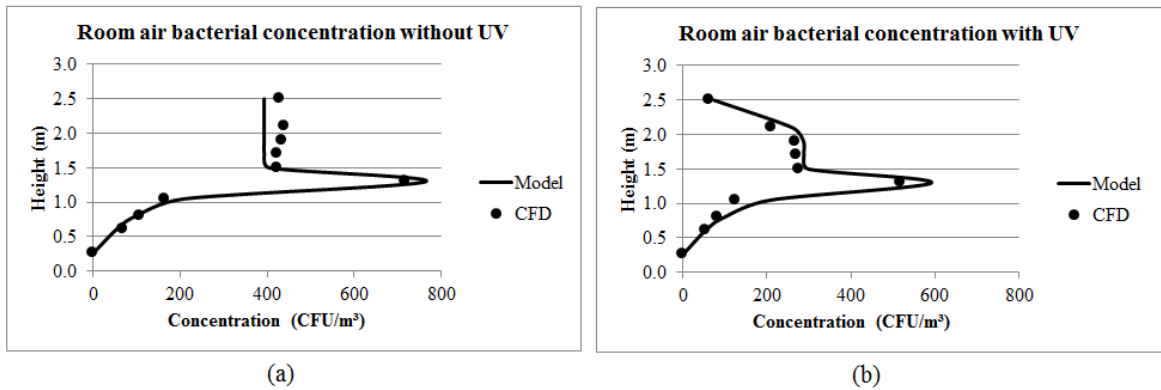


Fig. 17: Plots of the results using the multi-layer model and the CFD simulation predictions of bacteria concentrations as a function of height for room air (a) without use of UV and (b) with use of UV.

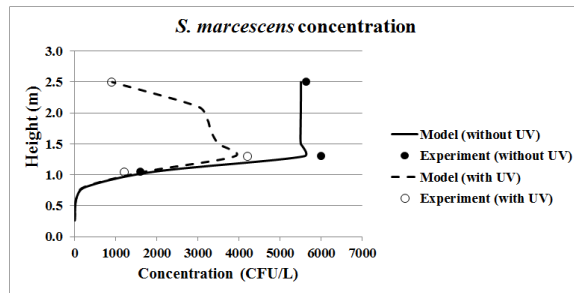
The simplified multi-layer model captures well the variations and the stratified exhalations due to the flow locking in the temperature gradient (Nielsen et al., 2012). The higher bacteria concentration occurs in the layer of stratification height being the

layer receiving both upward and downward mass fluxes through convective transport of bacteria. The *CFD* model is meant to determine the contaminant concentration in the air surrounding the occupants lumped in the breathing layer and not the concentration in the micro-inhalation zone. The transport processes in the breathing flow and between two people are not within the scope of this work. The indoor air quality is assessed based on the concentration in the surrounding air that is entrained to inhalation zone of a healthy occupant.

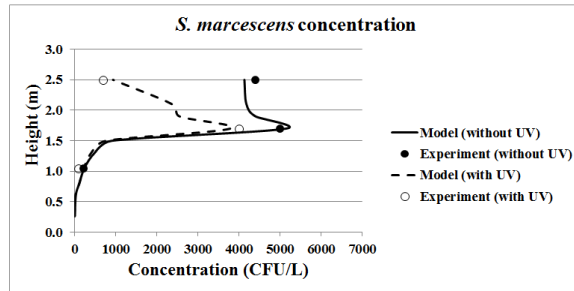
The plot shows that the model results are in good agreement with *CFD* results with a maximum relative error of 13% when UV is not used and 16% when UV is used.

3. Experimental Validation of the extended simplified model (for small droplets)

The values of airborne *S. marcescens* concentrations experimentally found using Eq. 13 compared well with those obtained from the mathematical model with maximal relative error of about 11% (Fig. 18).



(a)



(b)

Fig. 18: Comparative plot of measurements and model predictions for *S. marcescens* concentrations for (a) $m_s = 0.11$ kg/s and (b) $m_s = 0.22$ kg/s

However, a maximal relative error of 13% is found when the deposition is not included in the modeling.

More improvement on the model prediction accuracy is expected for larger particles where the effects of gravitational settling and deposition might be significant. Although the simulation is run for small droplets where the deposition effect is minimal, the model is able to give reasonable predictions of airborne bacteria concentration at different heights in the room. It can then be confirmed that the particle deposition is well estimated. The plots also show that for higher supply air flow rate the stratification in bacteria concentration created in *DV* flows occurs at higher level of the room. This is consistent with the findings of Habchi et al. (2014) and can be explained by the stronger opposition to particle settling.

The model is also able to predict reasonably the efficacy of the upper room *UVGI* since the relative error between the predicted and measured killing rates did not exceed 10%.

4. Experimental Validation of the CFD Model for Bacteria Deposition (for small droplets)

To evaluate the bacteria deposition in the room, the value from colony counting at each location is normalized by dividing it by the set experimental average. It is assumed that each *CFU* arises from a single viable microorganism. Fig. 19 shows a sample set of petri plates after incubation for one pair of experiments (with and without *UV*) with supply air flow rate 0.11 kg/s, supply temperature 20.6°C, chilled ceiling temperature 18.3°C, and bacteria atomization flow rate 12L/min.

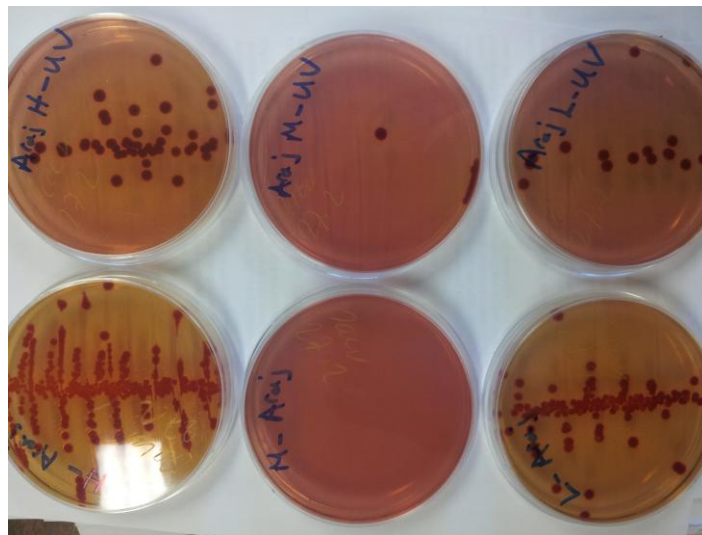
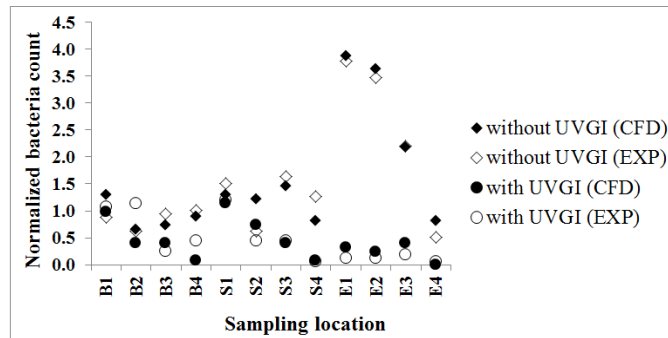


Fig. 19: Petri plates after incubation for one pair of experiments. The normalized bacteria count at a certain location *i* can be described by the following formula:

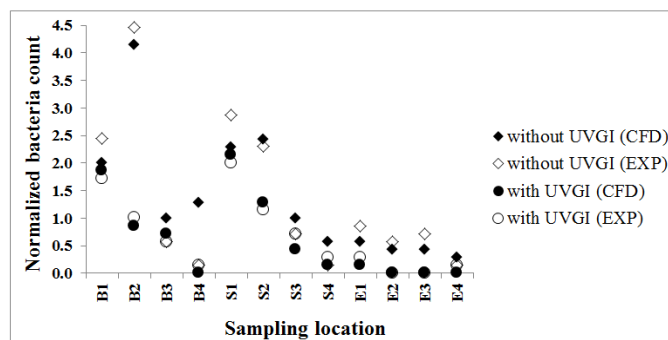
$$\bar{c}_i = \frac{c_i}{\frac{1}{n} \sum_{j=1}^n c_j} \quad (32)$$

where n is the total number of petri dishes.

A comparable normalization approach is adopted in analyzing simulation results to enable direct comparison between *CFD* and experimental spatial deposition patterns. Normalized experimental deposition values are presented together with *CFD* predictions at the twelve sampling plates are shown in Fig. 20. The *CFD* predictions of the number of droplet nuclei deposited on the petri plates are in good agreement with the *CFU* counts obtained experimentally with a relative error less than 15% at most of the sampling points.



(a)



(b)

Fig. 20: Comparison between experimental data and numerical bacteria deposition with and without the use of UVGI for (a) $m_s = 0.11$ kg/s and (b) $m_s = 0.22$ kg/s

The distribution map of *S. marcescens* on the sampling plane (V) predicted by the *CFD* simulations of Experiments I and II are shown in Fig. 21. The plots show that the use of two 18 W UVC lamps reduced remarkably the bacteria concentration in the room. The transmission of bacteria from the source to distant occupants is reduced as well.

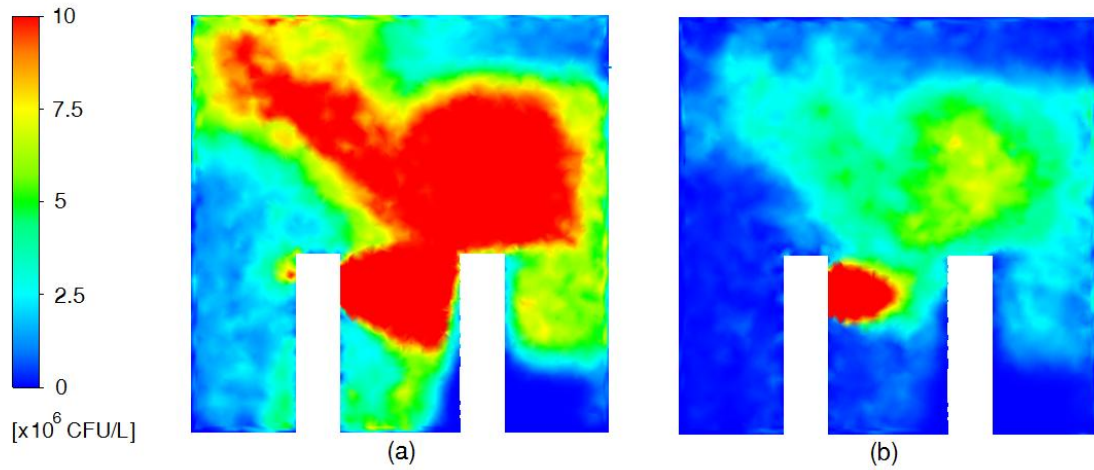
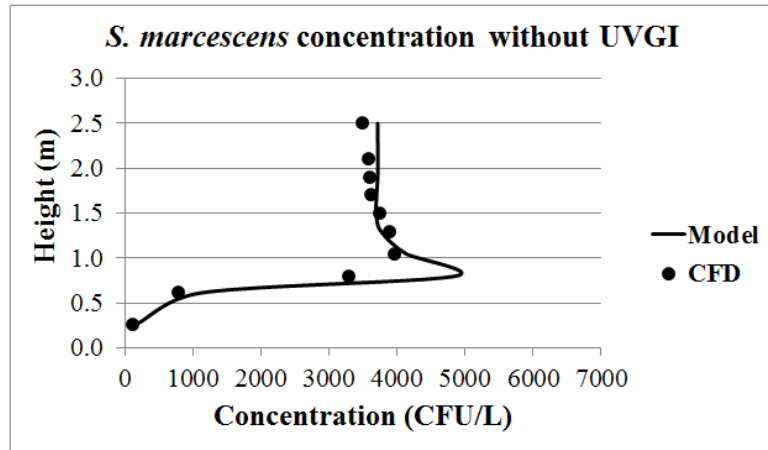


Fig. 21: *S. marcescens* concentration contour plots on the sampling plane for $m_s = 0.11$ kg/s (a) when UVGI is OFF and (b) when UVGI is ON

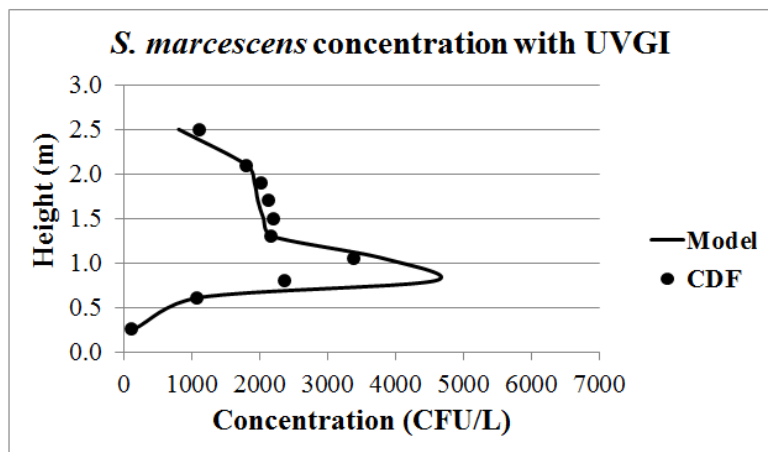
5. *CFD Substantiation of the Simplified Model (for large droplets)*

The experimentally validated *CFD* model is reliable in predicting the deposition of pathogen-carrying particles of different sizes. It can then be used to substantiate the mathematical model for the case of large particles. For this reason, experimental scenarios 1 and 2 are simulated using the *CFD* and mathematical model using a particle size of 20 μm (equilibrium diameter) and maintaining the other simulation parameters unchanged. The predictions of airborne bacteria from the two models are then compared and shown in Fig. 22 where good agreement with maximal relative error of 10% is obtained. It can be concluded that the mathematical model is able to predict reasonably the transport of pathogens carried by large droplets as well.

The comparison of the results obtained from the model not including the deposition effects with the *CFD* results for large droplets of 20 μm showed relative error up to 19%.



(a)



(b)

Fig. 22: Plots of bacteria concentration using the multi-layer model and the *CFD* simulation predictions as a function of height for room air (a) without the use of *UVGI* and (b) with the use of *UVGI*.

6. Effect of the Droplet Size

In order to study the effect of the droplet size on the pathogen transport in *UVGI* spaces conditioned by *CC/DV* system, the validated model is applied on the same experimental room for 4 different droplet equilibrium diameters: 2.5 μm , 10 μm , 15 μm , and 20 μm . The simulations runs are performed with and without the use of *UVGI* for

DV flow rate of 0.11 kg/s and bacteria emission rate of 1400 CFU/min from an infected person by talking and coughing. The variations of bacteria concentration with height and droplet equilibrium size are shown in Fig. 23.

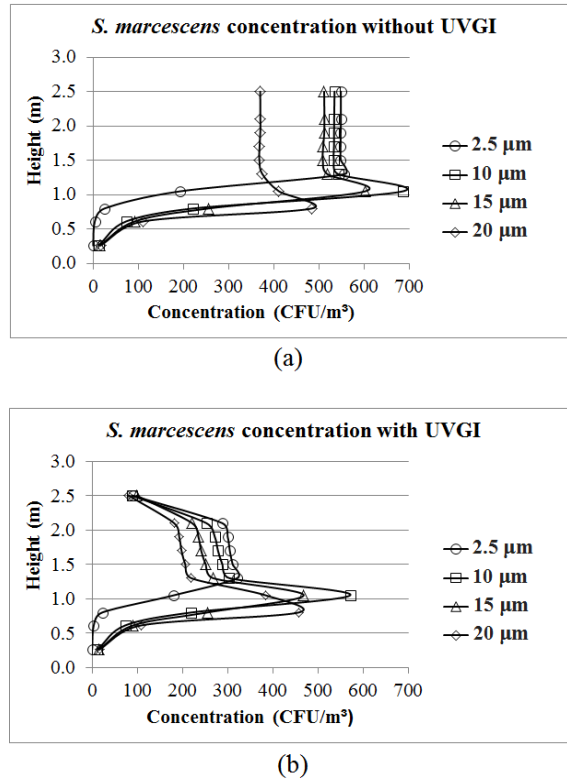


Fig. 23: Variations of bacteria concentration with height for droplet sizes 2.5, 10, 15, and 20 μm with and without the use of *UVGI*

As the droplet diameter increases, the effect of gravitational settling increases and results in a drop in the exhaust concentration. Moreover, the maximal bacteria concentration increases with the droplet diameter for droplet size up to 10 μm. For larger droplets, settling onto floor and other horizontal surfaces occurs quickly, and the maximal bacteria concentration begins to decrease when the droplet size exceeds 10 μm. The plots also show that the maximal concentration occurs at the stratification height for droplet size 2.5 μm and below this level for larger droplets. This finding can be explained by the increase in the gravitational settling that opposes the upward flow below the stratification level. In this case, unhealthy air quality is likely to occur in the

occupied zone and the return air mixing ratio should be at its minimum. The use of upper room *UVGI* is then highly recommended to allow higher fractions of return air and then achieve more energy savings on the system. Results also show that the disinfection rate in the upper zone decreases from 88% to 78% as the size of pathogen-carrying particles increases from 2.5 μm to 20 μm . This can be explained by the fact that more bacteria were removed by deposition of large carrying particles, which reduces the percentage of bacteria removed by *UV* irradiation.

CHAPTER IX

CASE STUDIES

A. Case Study 1 (horizontal air localization system)

The validated *CFD* model is used to evaluate the air quality in an office space in Beirut with dimensions of 6 m (L) × 6 m (W) × 2.7 m (H) equipped with localized zonal air distribution system that can recirculates the return air as shown in Fig. 24.

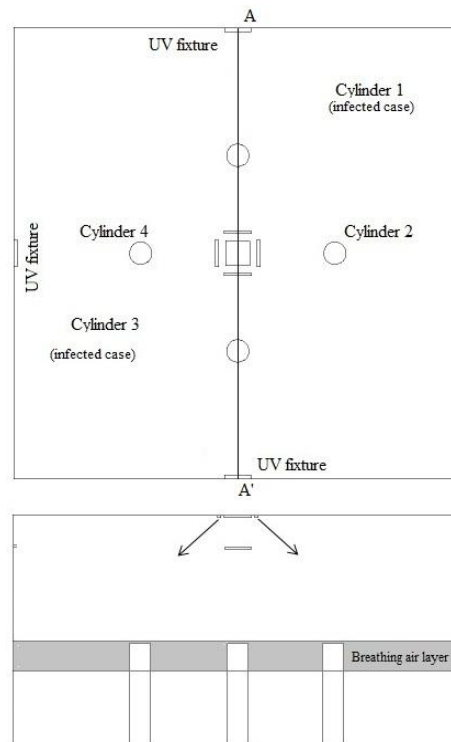


Fig. 24: Schematics of the office space (A) side view and (B) top view.

The aim of the case study is to examine if the use of UVGI not only offers protection within the zone, but also contributed to energy savings by reducing need fresh air fraction in supply fraction to meet the WHO standard (1988). The office

consists of two external walls with two partitions and is considered to be located above a conditioned space. The outdoor conditions during operational hours varied between 22 °C to 31°C in June, 24 °C to 32 °C in July, and 24 °C to 33 °C in August. The load change due to variation in outdoor temperature is less than 10%.

It is assumed that during the working hours (8:00-17:00), four occupants with two infected are regularly present in the office. Each occupant is simulated by a heated cylinder of height 1.2 m and diameter 0.3 m each of sensible load 100 W and CO₂ emission rate 0.6 L/min. Two of the occupants (cylinders 1 and 3) are infected and assumed to emit each 1,400 CFU/min of *S. marcescens*. Three louvered UV lamps with variable intensity and same configuration as used in the experimental CC/DV room described in Chapter 7. The use of louvers ensures safe UV irradiance levels in the occupied zone where the UV irradiance should not exceed the permissible limit of 0.002 W/m² based on 8 hours of continuous exposure to prevent any eye and skin injuries of occupants (American Conference of Governmental Industrial Hygienists, 2012).

Air is supplied at a temperature of 16 °C at air flow rate of 0.033 m³/s per slot supply jet at an angle 45° with the vertical. The case study space is simulated for the peak hour (15:00) using the validated CFD. The simulations will predict the volume-averaged CO₂ and *S. marcescens* concentrations in the breathing layer. The use of return air in the air distribution system results in energy savings, but is constrained by the IAQ standards (ASHRAE Standard 62.1-2014; WHO, 1988¹). Therefore, numerous simulations are performed without UVGI while changing the mixing ratio and keeping the supply conditions unchanged to identify the critical mixing ratio for both CO₂ and bacteria concentrations. An additional set of simulations is performed in order to

determine the minimal *UV* output that should be delivered to the space to maintain the acceptable air quality at maximum return mixing ratio.

1. Results without the Use of *UVGI*

Fig. 25 shows the variations of C/C_{max} in terms of mixing ratio where C is the species concentration in the breathing air layer and C_{max} is its standard limit value.

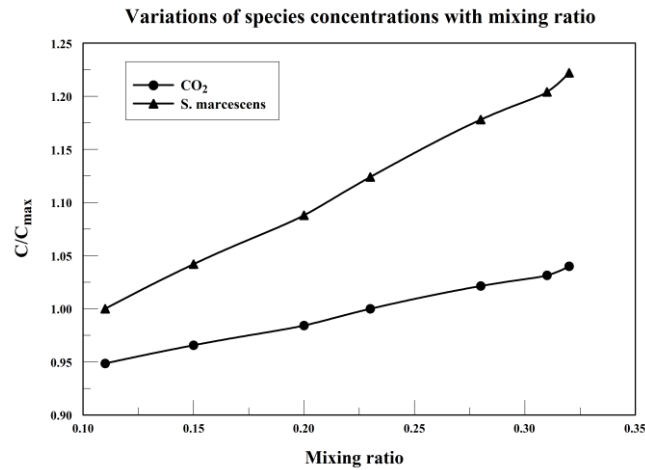


Fig. 25: Variations of C/C_{max} for both CO_2 and *S. marcescens* with their respective return air mixing ratios.

Results indicate that the concentration of 700 ppm CO_2 in the breathing air layer is obtained for a mixing ratio $x = 0.23$, whereas the bacterial concentration of 500 CFU/m^3 is obtained for a mixing ratio of $x = 0.11$. Therefore, the use of *UVGI* is strongly recommended to maintain an acceptable level of bacteria concentration in the breathing air layer while still using the maximal mixing ratio of 0.23. In addition, Fig. 26 shows the *S. marcescens* distributions on the vertical cut plane (A-A') for the case of (a) 100% fresh air and cases of critical mixing ratios of (b) 11% for the bacteria concentrations and (c) 23% for CO_2 .

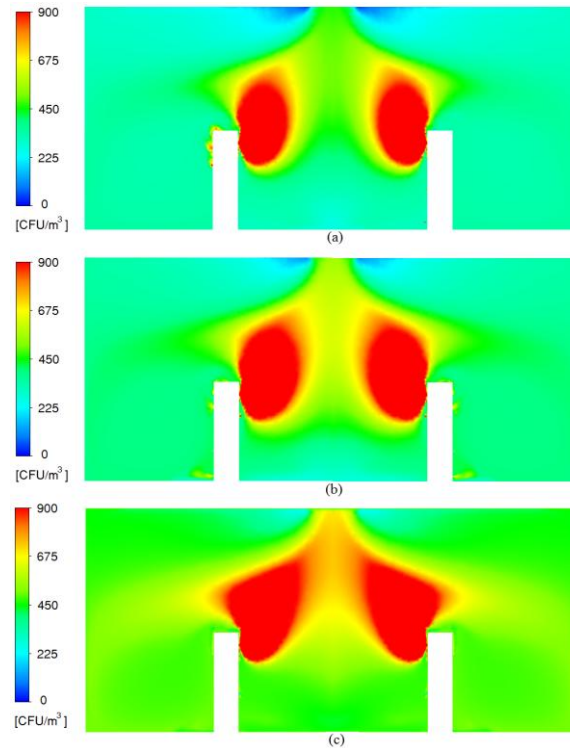


Fig. 26: *S. marcescens* distribution for (A) 100% fresh air, (B) 11% return mixing ratio, and (c) 23% return mixing ratio.

2. Results with the Use of UVGI

The simulation of the space for the peak hour with 23% return air (critical mixing ratio for CO₂ requirement) showed that the bacterial concentration in the breathing level is 592 *CFU/m*³, which does not satisfy the WHO requirement of 500 *CFU/m*³ limit for bacterial concentration. The use of upper-room *UVGI* is meant to reduce the bacterial limit to safe level without any additional energy consumption on the air conditioning system associated with increasing fresh air fraction. Several *CFD* simulations of the space with the three *UV* lamps operated are performed while changing the *UV* output from one lamp. Results showed that *S. marcescens* concentration in the breathing layer takes the standard limit value of 500 *CFU/m*³ when a total of 15 W *UV* is delivered to the space. The bacteria distribution field in this case

is shown in Fig. 27 which resembles the concentration field of bacteria for the case of 11% mixing ratio but without *UV*.

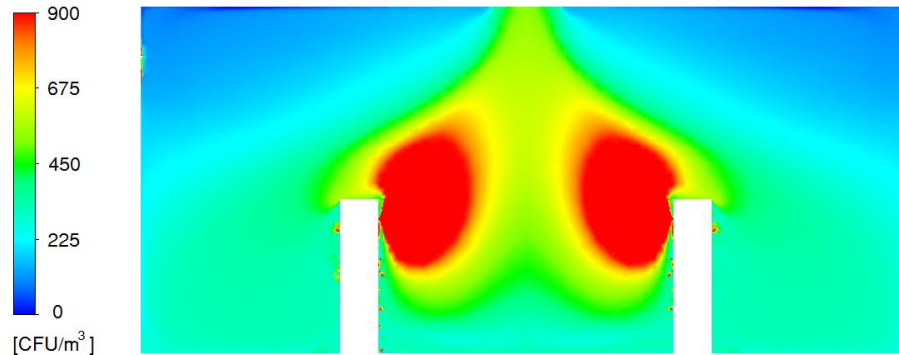


Fig. 27: Contour plots of *S. marcescens* concentration field for $x = 0.23$ when 15 W UV is delivered to the space.

3. Energy Analysis

The use of upper-room *UVGI* for reducing bacterial concentrations in occupied spaces is more economical than increasing the ventilation rate. Without the use of *UVGI*, the critical mixing ratio of 23% would have been decreased to 11% to establish healthy air quality in the breathing layer. This will result in additional energy consumption on the cooling system while same air quality can be obtained with minimum additional cost using the upper-room *UGVI*. Fig. 28 shows a comparative plot of the electrical power consumption of the localized air-conditioning system during the peak load time on typical days of June (30°C, 70% RH), July (32°C, 70% RH), and August (33°C, 72% RH) for different scenarios.

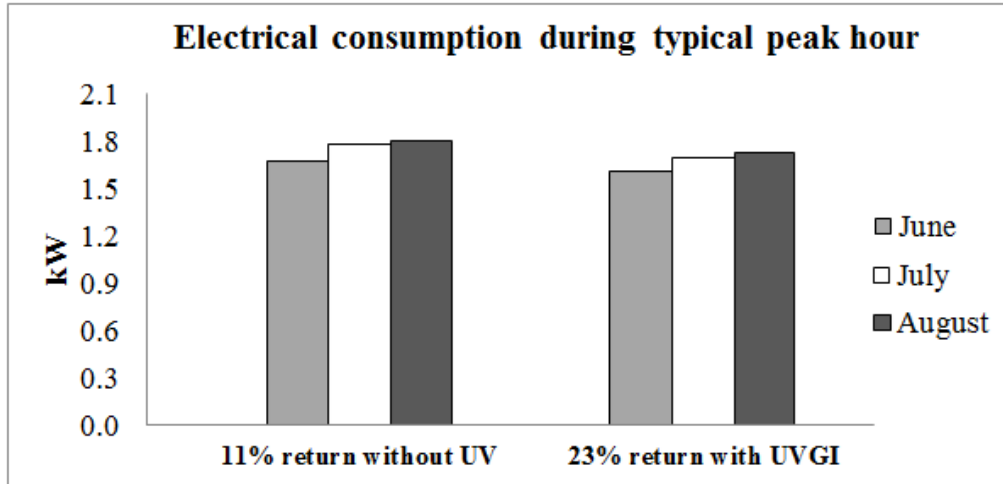


Fig. 28: Comparison of the horizontal air localization system electrical consumption during the peak hour on a typical day of June, July, and August for different mixing ratios.

Results show that when using higher return air ratio of 0.23 due to the presence of *UVGI*, the system consumes up to 7% less energy than the case of return air 0.11.

B. Case Study 2 (vertical air localization CC/DV system)

The validated plume multi-layer multi-zone bacteria transport model is used in a case study to show which standard is more stringent on the mixing ratio for the *CC/DV* system; i.e. the CO_2 concentration constraint not to exceed 700 ppm or the bacterial concentration constraint not to exceed 500 CFU /m³ in the breathing layers. The air quality is assessed in a 5 m × 5 m × 2.8 m health facility waiting room conditioned by mixed displacement ventilated and chilled ceiling in Beirut on a typical day of July. The room consists of two external walls (south and west oriented) with two partitions and is considered to be located above conditioned space at 25 °C. Three of the six occupants are infected and assumed to emit a total of 4,200 CFU/min of *S. aureus* by

breathing, sneezing, and coughing. The room is equipped with an upper-room *UVGI* system consisting of two louvered 12 W *UV* lamps placed symmetrically on the same wall at an elevation of 2.5 m. The supply and chilled ceiling temperatures are fixed at 19.5 °C and 17 °C respectively. The supply airflow conditions should be specified such that the stratification is above occupants' heads and temperature gradient does not exceed 2.5 °C/m. The supply flow rate also dictates the allowable mixing ratio for acceptable and healthy indoor air quality. Therefore, numerous simulations are performed with and without the use of *UVGI* to investigate the variations of critical mixing ratio for acceptable CO₂ concentration (not to exceed 700 ppm) and for satisfying the WHO requirement (bacterial concentration not to exceed 500 CFU/m³) in the occupied zone for different values of stratification height.

1. Results without the Use of UVGI:

The variation of critical mixing ratio is shown in Fig. 29 as a function of room stratification height which is strongly correlated with supply airflow rate (Ghaddar et al., 2008). The plots show that the critical maximum ratio for good indoor air quality is dictated by the bacteria concentration whose requirement is more restrictive than that of CO₂ concentration. The current room is simulated using the analytical model with a stratification height of 1.32 m. Results show that CO₂ concentration standard limit is obtained for a mixing ratio of 45%, and the corresponding bacteria concentration is 644 CFU/m³ in the breathing air region. The critical mixing ratio using bacteria concentration standard limit is determined to be 30%.

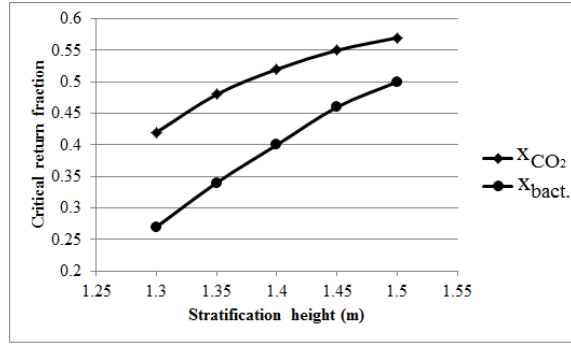


Fig. 29: Variation of critical mixing ratios with stratification height based CO_2 concentration and bacteria concentration standard limits in the occupied zone.

2. Results with the Use of UVGI:

Since the critical mixing ratio for CO_2 requirement does not satisfy the WHO requirement for bacterial concentration in the breathing region, the use of the upper-room *UVGI* is recommended to reduce the latter to 500 CFU/m^3 without any additional energy consumption on the air conditioning system. The average *UV* irradiance in the upper zone is predicted using the model of Wu et al. (2011) and is found to be 0.13 W/m^2 when the two lamps are ON and 0.07 W/m^2 when only one lamp is ON. The computed average irradiance in the occupied zone is 0.0008 W/m^2 when one lamp is ON and 0.0017 W/m^2 when the two lamps are ON. Both values are below the upper permissible limit of irradiance of 0.002 W/m^2 for human exposure (American Conference of Governmental Industrial Hygienists, 1999).

3. Energy Analysis

The plume multi-layer multi-zone model simulation is performed for the case when $H_s = 1.32\text{ m}$ while using a return air mixing ratio x at 45% (700 ppm of CO_2 is maintained in the breathing region) and with the two *UV* lamps ON. The resulting

bacterial concentration in the occupied zone air is reduced to 498 CFU/m³ compared to the value of 644 CFU/m³ found when the *UV* is OFF. A value of 540 CFU/m³ is found when one lamp is ON. Therefore, the two germicidal lamps with total *UV* output of 24W should be operated to obtain the desired level of bacteria concentrations. Note that these results are not accounting for any bacteria loss resulting from surface deposition in the air ducting system or bacteria gain due to bacteria growth in supply system. On the other hand, more than 24 W of *UV* is required to obtain the same air quality if in-duct *UVGI* is meant to be used due to the short exposure time of air to *UV* in the supply duct.

The simplified model determines that *S. aureus* killing rate of the in-duct *UVGI* when used should be about 57% to achieve the 498 CFU/m³ obtained using 24W of upper-room *UVGI*. The corresponding *UV* irradiance assumed uniform is calculated using the supply airflow rate (0.21kg/s), geometry of the supply duct (cross section 0.61m×0.61m and length 0.9m) and *S. aureus* susceptibility to *UV* and it is found to be 1.29W/m with an average residence time of 1.88 s. The required *UV* output is estimated to be about 180W using the work of Lau et al. (2012) that experimentally measured the *UV* irradiance in a similar duct assumed to have same *UV* reflectance and diffusion properties. The average *UV* irradiance is about 1.31W/m² which is quite close to the irradiance required in the current case.

The use of upper-room *UVGI* for reducing bacterial concentrations in occupied spaces is an economical substitute to increasing fresh air intake at the supply. If the upper-room *UVGI* is not used in the current case, the critical mixing ratio of 45% should be decreased to 30% to establish healthy air quality in the breathing air region. This will result in additional energy consumption on the cooling system while same air quality can be obtained with minimum cooling cost using the upper-room *UGVI*.

Fig. 30 shows a comparative plot of the electrical consumption of the *CC/DV* system when operated with 30% return air without the use of *UV*, and 45% return air with the use of upper-room and in-duct *UVGI*.

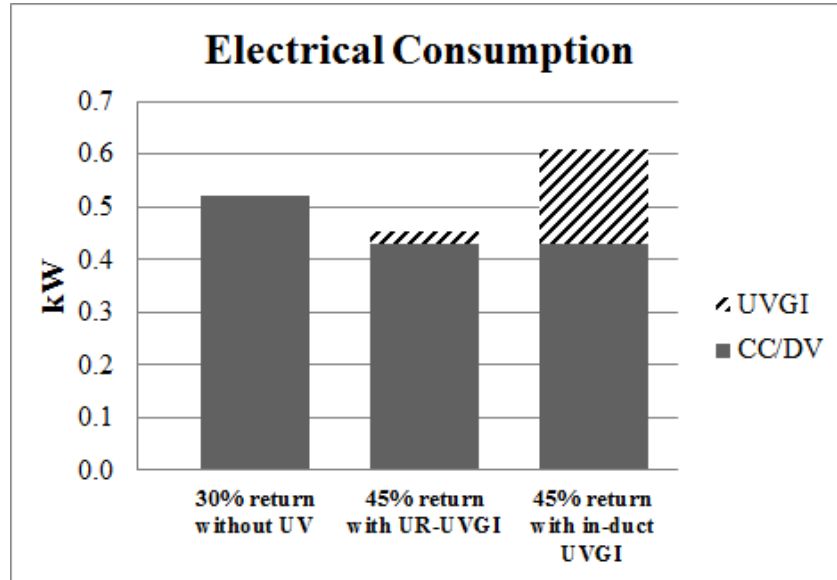


Fig. 30: Comparison of the system electrical consumption for different mixing ratios and UVGI setups

Results show that most efficient method for achieving acceptable *IAQ* is to use *UR-UVGI* to allow the higher return air ratio of 0.45. This optimal setting yields energy savings up to 12% when compared to the case of return ratio 0.30 without the use of *UV* and up to 26% when compared to the case of in-duct UVGI system.

CHAPTER X

CONCLUSIONS AND FUTURE WORK

A CFD model using Eulerian approach is developed and experimentally validated to predict the airborne bacteria transport in horizontal and vertical air localization systems with UR-UVGI. The developed model can simulate the return air recirculation and predict the CO₂ and bacteria distributions in the space for different mixing ratios and UV outputs. The CFD-UV model is also validated using published experimental data.

A simplified plume multi-layer model is also developed for airborne bacteria transport at different droplet sizes in rooms conditioned by DV/CC system and equipped with upper room UVGI louvered lamps. The model divided the room into different zones depending on mechanism of bacterial transport for buoyant, partially mixed, and fully mixed regions. The model is validated by experimentation for small droplets and then substantiated using CFD for large droplets. Moreover, the Lagrangian tracking model is used in CFD simulations to predict the bacteria settling in CC/DV system. Results showed good agreement between the settling predictions and measured bacteria CFU on settling petri plates. The simplified model is then used to study the effect of droplet size on bacteria distribution and UR-UVGI performance.

The validated CFD model is applied to a case study on horizontal air localization system recirculating return air, whereas the simplified model is implemented for a case study on CC/ mixed DV system. The effect of return air mixing

ratio on indoor air quality and energy performance is investigated. This study comes up with the following conclusions:

- The developed *CFD* model can be used to determine the critical return air mixing ratio for *IAQ* standard for CO_2 concentration and the minimal *UV* output to deliver to space to achieve good and healthy *IAQ* at minimum energy consumption. A case study on horizontal air localization system with a constant generation of 1400 CFU/min showed that a return ratio of 0.23 can be tolerated if a minimal UV output of 15 W is delivered to the space. This scenario results in energy consumption less by 7% than the case of return air of 0.11 critical for CO_2 standard limit at the breathing layer.
- The horizontal air localization system with mixed supply air fails to protect the occupants within one zone from cross-infection. However, relatively high mixing ratio may be allowed when upper room *UVGI* is used and about 15% energy savings can be achieved.
- The use return air in CC/DV rooms enhances the economic viability of this system, but it is constrained by air quality requirements for occupants based on maximum allowable level of bacteria (100 CFU/m³ for hospitals and 500 CFU/m³ for offices recommended by WHO, 1988) and CO_2 concentrations (700 ppm recommended by ASHRAE, 2014)
- It is the bacteria and not the CO_2 concentration at the breathing level that determines the indoor air quality in CC/DV systems since the CFU count requirement has been proven more restrictive than that of CO_2 .

- The use of upper room UVGI in CC/DV system helps to effectively increase the return air ratio and then optimize the energy performance of the system. The critical return air ratio for good and healthy IAQ increased from 30% to 45% when UR-UVGI was used, which resulted in 7% energy savings. However, the use of in-duct UVGI does not offer any economic edge for the CC/DV system.
- The advantage of mixed DV systems when using UR-UVGI is that the upward airflow in DV systems transports pathogens to the upper irradiated zone where they receive sufficient UV dose because of long residence time due to air recirculation in that zone. The return air is then effectively disinfected before being used with significant fraction in the supply upstream without violating the CFU count requirement, and at relatively low UV cost when compared to in-duct UVGI systems that have less economic viability.
- The maximal airborne bacteria concentration occurs at the stratification level in CC/DV rooms for droplet nuclei size, and below this level for larger droplets. It can be then concluded the CC/DV is capable of protecting occupants from airborne disease transmission, but not from droplet disease transmission since the gravitational settling of large droplets results in higher concentrations in the occupied zone.
- The performance of upper room UVGI is also affected by the droplet size since larger portion of bacteria will be removed by deposition in case of large pathogen carriers. The study shows that the UVGI disinfection rate in the upper zone dropped from 88% to 78% as the equilibrium diameter of the droplets increases from 2.5 μm to 20 μm .

The following can be viewed as future work:

- CFD evaluation and comparison of UR-UVGI effectiveness in the horizontal and vertical localized air conditioning systems at the same UV output, ventilation rate and bacteria type. Although the current work shows that both air distribution systems have economic advantage on the conventional HVAC systems, the outcomes of the suggested comparison will help decide on the system that provides better thermal comfort and economic edge.
- Studying the effect of chilled ceiling temperature on the performance of UR-UVGI in CC/DV spaces. The CC temperature affects air recirculation in the upper zone and then can be used to optimize the bacteria residence time in the UV zone for achieving maximum disinfection.
- Developing design charts for UR-UVGI systems that can correlate the needed UV output with the bacteria generation rate per floor square meter, ventilation rate, and UV susceptibility of targeted bacteria.
- Modeling the performance of the Mobile Room Sanitizer (MRS) that is a UVGI unit used to disinfect in short time a patient room in hospital before the next occupant is admitted. Here, the equipment and indoor surfaces are targeted to prevent disease transmission by contact. The suggested modeling work can be used to determine the minimal UV output needed for effective disinfection during a given time interval. This will optimize the selection of the UV lamps to achieve required cleaning at minimal energy cost. The study may also consider the effect of UV light on furniture and equipment, and then stimulate the research to find protective measures when using MRS.

- Focusing on the human exhalation process to simulate more accurately the pathogen generation from humans in indoor environments. Although the steady simulation of the expiratory activities used in the current work has been considered acceptable in the literature, unsteady models can be developed to represent the periodicity of breathing and the impulse of coughing and sneezing. This will improve the predictions of UR-UVGI performance in providing healthy IAQ and reduce modeling discrepancies. Experimental Particle Image Velocimetry (PIV) work can be also performed to measure the exhaled flow for each expiratory activity and determine the size distribution of the emitted droplets.
- Consideration of pathogen concentration in the micro-inhalation zone by studying the complex geometry of the nose and other parts of the human face. Humans can be simulated by mannequin instead of cylinders. This will improve the assessment of thermal comfort and quality of the air that is immediately inhaled.
- Studying the use of carbon filters in the mixed DV supply upstream to reduce the CO₂ concentration in the supply air and their effects on the optimal return air mixing ratio.
- Consideration of Volatile Organic Compounds (VOCs) besides CO₂ and bioaerosols to obtain complete assessment of IAQ.
- Modeling the bacteria growth on the internal components of HVAC systems and correlating the growth rate with the microbiological quality of the air supplied by the contaminated systems to conditioned spaces. This will provide reliable

predictions of the bacteria generation rate from the biologically contaminated air distribution systems.

BIBLIOGRAPHY

American Conference of Governmental Industrial Hygienists. TLVs and BEIs. Cincinnati: ACGIH, 1999.

ANSYS Software. ANSYS14.5 © 2012 SAS IP, Inc.

Ariff, M., Salim, M.S., and Cheah, S.C. (2009). “Wall y^+ approach for dealing with turbulent flow over surface mounted cube: Part2 - High Reynolds number”, *Seventh International Conference on CFD in the Minerals and Process Industries CSIRO, Melbourne, Australia*, December 9-11, 2009

ASHRAE. ANSI/ASHRAE Standard 62.1-2014, *Ventilation for Acceptable Indoor Air Quality*. American Society of Heating, Air-Conditioning and Refrigeration Engineers, Inc. 2014.

ASHRAE. ASHRAE Standard 52.2-2012, Method of testing general ventilation air-cleaning devices for removal efficiency by particle size. Atlanta: American Society of Heating, Refrigerating and Air-conditioning Engineers, Inc. 2012.

ASHRAE. ASHRAE Standard 55-2013, Thermal environmental conditions for human occupancy. Atlanta: American Society of Heating, Refrigerating and Air-conditioning Engineers, Inc. 2013.

Ayoub M., Ghaddar N, and Ghali K. (2006). “Simplified thermal model of spaces cooled with combined positive displacement ventilation and chilled ceiling system.” *HVAC&R Research*, 12(4), 1005-1030..

Bahman, A., Chakroun, W., Saadeh, R., Ghali, K., and Ghaddar, N. (2008). “Performance comparison conventional and chilled ceiling/ displacement ventilation systems in Kuwait.” *ASHRAE Transactions*, 115 (2), 587-594.

Beggs, C.B. and Sleigh, P.A. (2002). "A quantitative method for evaluating the germicidal effect of upper room UV fields." *Journal of Aerosol Science*, 33 (12), 1681-1699.

Beggs, C., Kerr, K., Donnelly, J., Sleigh, P., Mara, D., and Cairns, G. (2000). "An engineering approach to the control of *Mycobacterium tuberculosis* and other airborne pathogens: a UK hospital based pilot study." *Trans.R.Soc.Trop.Med.Hyg.*, 94 (2), 141-146.

Behne, M. (1999). "Indoor air quality in rooms with cooled ceilings: mixing ventilation or rather displacement ventilation?" *Energy and Buildings*, 30(2),155-166.

Bolashikov, Z.D., and A.K. Melikov. (2009). " Methods for air cleaning and protection of occupants for airborne pathogens." *Building and Environment*, 44: 1378-1385.

Bourouiba, L., Dehandschoewercker, E., & Bush, J. W. (2014). "Violent expiratory events: on coughing and sneezing." *Journal of Fluid Mechanics*, 745: 537-563.

Brodka, K., Sowiak, M., Kozajda, A., Cyprowski, M., and Irena, S. S. (2012). "Biological contamination in office buildings related to ventilation/air conditioning system." *Med.Pr.*, 63(3), 303-315.

Chakroun, W., Ghali, K., and Ghaddar, N. (2011). "Air quality in rooms conditioned by chilled ceiling and mixed displacement ventilation for energy saving." *Energy Build.*, 43(10), 2684-2695.

Chao, C.Y.H, Wan, M.P., Morawska, L., Johnson, G.R, Ristovski, Z.D, Hargreaves, et al. (2009). " Characterization of expiration air jets and droplet size

distributions immediately at the mouth opening.” *Journal of Aerosol Science* , 40(2):122-133.

Chen, Q., and Srebric, J. (2000). “Simplified Diffuser Boundary Conditions for Numerical Room Airflow Models” Final Report for ASHRAE RP-1009, Department of Architecture, Massachusetts Institute of Technology, Cambridge, MA.

Chen, Q, and Xu, W. (1998). “A zero-equation turbulence model for indoor airflow simulation.” *Energy and Buildings*, 28:137–44.

Chmielewski, M., and Gieras, M. (2013). “Three-zonal Wall Function for k-ε Turbulence Models”. *CMST*, 19: 107-114.

Cho, K.J., Reponen, T., McKay, R., Dwivedi, A., Adhikari, A., Singh, U., Shukla, R., Jones, S., Jones, G., and Grinshpun, S.A. (2011) “Comparison of workplace protection factors for different biological contaminants.” *Journal of occupational and environmental hygiene* ,8(7): 417-425.

Cole, E.C., and Cook, C.E. (1998). “Characterization of infectious aerosols in health care facilities: an aid to effective engineering controls and preventive strategies.” *American Journal of Infection Control*, 26: 453-464.

Corbett, E. L., Watt, C. J., Walker, N., Maher, D., Williams, B. G., Raviglione, M. C., and Dye, C. (2003). "The growing burden of tuberculosis: global trends and interactions with the HIV epidemic." *Arch.Intern.Med.*, 163(9), 1009-1021.

Davis, Dulbecco, Eisen, Ginsberg, *Bacterial Physiology: Microbiology, Second Edition*, Maryland: Harper and Row, 1973: 96-97.

Duguid, J.P. (1946) "The size and duration of air-carriage of respiratory droplets and droplet-nuclei." *J. Hyg.*, 4:471–480.

Dunnett, S.J. (1994) "A numerical study of the factors affecting worker exposure to contaminant." *Aerosol Sci*, 25(Suppl.1):481–482.

Fairchild, C., and Stampfer, J. (1987). "Particle concentration in exhaled breath." *The American Industrial Hygiene Association Journal*, 48(11), 948-949.

Fennelly, K. P., Martyny, J. W., Fulton, K. E., Orme, I. M., Cave, D. M., and Heifets, L. B. (2004). "Cough-generated aerosols of *Mycobacterium tuberculosis*: a new method to study infectiousness." *American Journal of Respiratory and Critical Care Medicine*, 169(5), 604-609.

First, M., Rudnick, S. N., Banahan, K. F., Vincent, R. L., and Brickner, P. W. (2007). "Fundamental factors affecting upper-room ultraviolet germicidal irradiation—part I. Experimental." *Journal of Occupational and Environmental Hygiene*, 4(5), 321-331.

Gao, N.P, and Niu, J.L. (2007) "Modeling particle dispersion and deposition in indoor environments." *Atmospheric Environment* 41, 3862-3876.

Ghaddar, N., Saadeh, R., Ghali, K., and Keblawi, A. (2008). "Design Charts for Combined Chilled Ceiling Displacement Ventilation System." *ASHRAE Trans*, 114(2):574-587.

Ghali, K, Ghaddar, N, and Ayoub, M. (2007) "Chilled ceiling and displacement ventilation system: an opportunity for energy saving in Beirut." *International Journal of Energy Research*, 31:743-759.

Gold, E, and Nankervis, G.A. Cytomegalovirus. In: Evans, A. (ed.) *Viral Infections of Humans* 1989; pp 997–1002. New York, Plenum Medical Book Co.

Goodfellow H.D. (2001) "Industrial ventilation design guidebook." A Harcourt Science and Technology Company, San Diego, California, USA.

Gupta, J.K., Lin, C.H., and Chen, Q. (2010). "Characterizing exhaled airflow from breathing and talking." *Indoor Air*, 20: 31–39.

Gutierrez, J. (2011). "Correlation of Cough Frequency with Treatment Efficacy in Pulmonary Tuberculosis Patients in Lima, Peru." *Master's Theses*. Paper 199.

Habchi, C., Ghali, K., and Ghaddar, N. (2014). "A simplified mathematical model for predicting cross contamination in displacement ventilation air-conditioned spaces." *J. Aerosol Sci.*, 76:72-86.

Harris, L.G., Foster, S.J., and Richards, R.G. (2002). "An introduction to Staphylococcus aureus, and techniques for identifying and quantifying S. aureus adhesion to biomaterials: Review." *European Cells and Materials*, 4:39-60.

Hatch, M.T., and Wolochow H. (1969). "Bacterial survival: consequences of the airborne state", p.267-295. In R.L. Dimmick and A.B.Akers (ed.), An introduction to experimental aerobiology. Wiley-Interscience, New York.

Hathway, E., Noakes, C., Sleigh, P., and Fletcher, L. (2011). "CFD simulation of airborne pathogen transport due to human activities." *Build. Environ.*, 46(12), 2500-2511.

Heidarinejad, M., and Srebric, J. (2013). "Computational fluid dynamics modelling of UR–UVGI lamp effectiveness to promote disinfection of airborne microorganisms." *World Review of Science, Technology and Sustainable Development*, 10(1), 78-95.

Hugenholtz, P., and Fuerst, J. A. (1992). "Heterotrophic bacteria in an air-handling system." *Appl. Environ. Microbiol.*, 58(12), 3914-3920.

Ismail, S. H., and Leman, A. (2010). "Indoor air quality issues for non-industrial work place. *International Journal of Research & Reviews in Applied Sciences*, 5(3), 235-244.

Jacob, S. M., and Dranoff, J. S. (1970). "Light intensity profiles in a perfectly mixed photoreactor." *Aiche j.*, 16(3), 359-363.

Jaluria, Y. (1980) "Natural convection." Pergamon Press Oxford.

Jiang, W., and Reddy, T. A. (2007). "General methodology combining engineering optimization of primary HVAC&R plants with decision analysis methods—Part I: Deterministic analysis." *HVAC&R Research*, 13(1), 93-117.

Jo, W., and Lee, J. (2008). "Airborne fungal and bacterial levels associated with the use of automobile air conditioners or heaters, room air conditioners, and humidifiers." *Archives of Environmental & Occupational Health*, 63(3), 101-107.

Joubert, A., Laborde, J.C. , Bouilloux, L., Chazelet, S., and Thomas, D. (2011). "Modelling the pressure drop across HEPA filters during cake filtration in the presence of humidity." *Chemical Engineering Journal* 166: 616–623.

Kanaan, M., Ghaddar, N., Ghali, K., and Araj, G. (2014). "New airborne pathogen transport model for upper-room UVGI spaces conditioned by chilled ceiling and mixed displacement ventilation, Enhancing air quality and energy performance." *Energy Conversion and Management* 85:50-61.

Kanaan, M., Ghaddar, N., and Ghali, K. (2010). "Simplified model of contaminant dispersion in rooms conditioned by chilled-ceiling displacement ventilation system." *HVAC&R Research*, 16(6), 765-783.

Kayumba, A.V., Bråtveit, M., Mashalla, Y., Baste, V., Eduard, W., and Moen, B.E. (2009) "Working conditions and exposure to dust and bioaerosols in sisal processing factories in Tanzania." *Journal of occupational and environmental hygiene*, 6(3):165-173.

Kearns, A. M., Barrett, A., Marshall, C., Freeman, R., Magee, J. G., Bourke, S. J., and Steward, M. (2000). "Epidemiology and molecular typing of an outbreak of tuberculosis in a hostel for homeless men." *J.Clin.Pathol.*, 53(2), 122-124.

Keblawi, A., Ghaddar, N., and Ghali, K. (2011). "Model-based optimal supervisory control of chilled ceiling displacement ventilation system." *Energy and Buildings*, 43:1359-1370.

Keblawi, A., Ghaddar, N., Ghali, K., and Jensen, L. (2009). "Chilled ceiling displacement ventilation design charts correlations to employ in optimized system operation for feasible load ranges." *Energy Build.*, 41(11), 1155-1164.

Kemp, P., Neumeister-Kemp, H., Lysek, G., and Murray, F. (2001). "Survival and growth of micro-organisms on air filtration media during initial loading." *Atmos.Environ.*, 35(28), 4739-4749.

King, M.F., Noakes, C.J., Sleight, P.A, Camargo-Valero, M.A. (2012). "Bioaerosol deposition in single and two-bed hospital rooms: A numerical and experimental study." *Building and Environment*, 436-447.

Ko, G., First, M., and Burge, H. (2000). "Influence of relative humidity on particle size and UV sensitivity of *Serratia marcescens* and *Mycobacterium bovis BCG* aerosols." *Tubercle Lung Dis.*, 80(4), 217-228.

Kowalski, W. (2009) *Ultraviolet Germicidal Irradiation Handbook*, 73 DOI 10.1007/978-3-642-01999-9_4, C Springer-Verlag Berlin Heidelberg 2009.

Kowalski, W., Bahnfleth, W., and Hernandez, M. (2009). "A genomic model for predicting the ultraviolet susceptibility of viruses." *IUVA News*, 11(2), 15-28.

Kowalski, W., Bahnfleth, W., and Rosenberger, J. (2003). "Dimensional analysis of UVGI air disinfection systems." *HVAC&R Research*, 9(3), 347-363.

Kuhn, H., Braslavsky, S., and Schmidt, R. (2004). "Chemical actinometry (IUPAC technical report)." *Pure and Applied Chemistry*, 76(12), 2105-2146.

Kujundzic, E., Hernandez, M., and Miller, S.L. (2007) "Ultraviolet germicidal irradiation inactivation of airborne fungal spores and bacteria in upper-room air and HVAC in-duct configurations." *Journal of Environmental Engineering and Science* 6:1-9.

Lai, A.C.K, Nazaroff, W.W. (2000). "Modeling indoor particle deposition from turbulent flow onto smooth surfaces." *J. Aerosol Sci.*, 31(4), 463-476.

Lau, J., Bahnfleth, W., Mistrick, R., Kompare, D. (2012). "Ultraviolet irradiance measurement and modeling for evaluating the effectiveness of in-duct ultraviolet germicidal irradiation devices." *HVAC&R Research*, 18:626-642.

Lindsley, W.G., King, W.P., Thewlis, R.E., Reynolds, J.S., Panday, K., Cao, G., and Szalajda, J. V. (2012). "Dispersion and exposure to a cough-generated aerosol in a simulated medical examination room." *Journal of occupational and environmental hygiene* , 9(12), 681-690.

Lo, L. J., and Novoselac, A. (2010). "Localized air-conditioning with occupancy control in an open office." *Energy Build.*, 42(7), 1120-1128.

Loudon, R.G., and Roberts, R.M. (1967). "Relation between the airborne diameters of respiratory droplets and the diameter of the stains left after recovery." *Nature*, 213:95–96.

Mahajan, R. P., Singh, P., Murty, G. E., and Aitkenhead, A. R. (1994). "Relationship between expired lung volume, peak flow rate and peak velocity time during a voluntary cough manoeuvre." *Br.J.Anaesth.*, 72(3), 298-301.

Mandal, J., and Brandl, H. (2011). "Bioaerosols in Indoor Environment-A Review with Special Reference to Residential and Occupational Locations." *Open Environmental & Biological Monitoring Journal*, 4:83-96.

McCluskey, R., Sandin, R., and Greene, J. (1996). "Detection of airborne cytomegalovirus in hospital rooms of immunocompromised patients." *Journal of virological methods*, 56(1), 115-118.

Miller, F.J., Gardner, D.E., Graham, J.A., Lee Jr., R.A., Wilson, W.A., and Bachmann, J.D. (1979). "Size considerations for establishing a standard for inhalable particles." *Journal of the Air Pollution Control Association*, 29(6): 610-615.

Miller, S. L., and Macher, J. M. (2000). "Evaluation of a methodology for quantifying the effect of room air ultraviolet germicidal irradiation on airborne bacteria." *Aerosol.Sci.Technol.*, 33(3), 274-295.

Miller, S., Xu, P., Peccia, J., Fabian, P., and Hernandez, M. (1999). "Effects of ultraviolet germicidal irradiation of room air on airborne bacteria and mycobacteria." *Indoor Air*, 665-670.

Modest, M.F. (1993). Radiative Heat Transfer. New York: McGraw-Hill.

Morawska, L. (2006). "Droplet fate in indoor environments, or can we prevent the spread of infection?" *Indoor Air*, 16(5), 335-347.

Morey, P., Otten, J., Burge, H., Chatigny, M., Feeley, J., LaForce, F., and Peterson, K. (1986). "Airborne viable microorganisms in office environments: sampling protocol and analytical procedures." *Applied Industrial Hygiene*, 1 R19-R23.

Mossolly, M., Ghali, K., Ghaddar, N., and Jensen, L. (2008). "Optimized Operation of Combined Chilled Ceiling Displacement Ventilation System Using Genetic Algorithm." *ASHRAE Trans*, 114(2), 541-554.

Mui, K.W., Wong, L.T., Wu, C.L., and Lai, A.C.K. (2009) "Numerical modeling of exhaled dispersion and mixing in indoor environments", *Journal of Hazardous Materials*, 167(1-3), 736-744.

Mundt, E. (1996) "The performance of displacement ventilation system." Ph.D Thesis, Sweden: Royal Institute of Technology.

Nardell, E. A., Bucher, S. J., Brickner, P. W., Wang, C., Vincent, R. L., Becan-McBride, K., James, M. A., Michael, M., and Wright, J. D. (2008). "Safety of upper-room ultraviolet germicidal air disinfection for room occupants: results from the Tuberculosis Ultraviolet Shelter Study." *Public Health Rep.*, 123(1), 52-60.

Nicas, M., and Miller, S.L. (1999). "A multi-zone model evaluation of the efficacy of upper-room air ultraviolet germicidal irradiation." *Appl Occup Environ Hygiene*, 14:317-328.

Nicas, M., Nazaroff, W., and Hubbard, A. (2005). "Toward understanding the risk of secondary airborne infection: emission of respirable pathogens." *Journal of occupational and environmental hygiene*, 2:143-154.

Nielsen P.V. (2007). "Analysis and Design of Room Air Distribution Systems." *HVAC & R Research* 13(6): 987 – 997.

Nielsen, P.V., Jensen, R. L., Litewnicki, M., and Zajac, J. J. (2009). "Experiments on the microenvironment and breathing of a person in isothermal and stratified surroundings." *The International Conference & Exhibition of Healthy Buildings*.

Nielsen, P.V, Olmedo, I., Ruiz de Adana, M., Grzelecki, P., and Jensen, R.L. "Airborne cross-infection risk between two people standing in surroundings with a vertical temperature gradient." *HVAC&R Research*, 18:552-561.

Noakes, C., Beggs, C., and Sleight, P. (2004). "Modelling the performance of upper room ultraviolet germicidal irradiation devices in ventilated rooms: comparison of analytical and CFD methods." *Indoor and Built Environment*, 13(6), 477-488.

Noakes, C., Sleight, P., Fletcher, L., and Beggs, C. (2006). "Use of CFD modeling to optimize the design of upper-room UVGI disinfection systems for ventilated rooms." *Indoor and Built Environment*, 15 (4), 347-356.

Oh, M.S., Ahn, J.H., Kim, D.W., Jang, D. S., and Kim, Y. (2014). "Thermal comfort and energy saving in a vehicle compartment using a localized air-conditioning system." *Applied Energy*: 133, 14-21.

Papineni, R.S., Rosenthal, F.S. (1997) "The size distribution of droplets in the exhaled breath of healthy human subjects", *Journal of Aerosol Medicine: Deposition, Clearance, and Effects in the Lung*, 10 (2), 105-116.

Peccia, J., Werth, H. M., Miller, S., and Hernandez, M. (2001). "Effects of relative humidity on the ultraviolet induced inactivation of airborne bacteria." *Aerosol.Sci.Technol.*, 35(3), 728-740.

Qualls, R. G., and Johnson, J. D. (1985). "Modeling and efficiency of ultraviolet disinfection systems." *Water Res.*, 19(8), 1039-1046.

Rahn, R. O., Xu, P., and Miller, S. L. (1999). "Dosimetry of room-air germicidal (254 nm) radiation using spherical actinometry." *Photochem.Photobiol.*, 70(3), 314-318.

Riley R.L. (1957). "Aerial dissemination of pulmonary tuberculosis." *American review of tuberculosis*, 76(6), 931-941.

Riley, R. L., and Kaufman, J. E. (1972). "Effect of relative humidity on the inactivation of airborne *Serratia marcescens* by ultraviolet radiation." *Appl.Microbiol.*, 23(6), 1113-1120.

Riley, R.L., Permutt, S., Kaufman, J.E. (1971). "Convection, air mixing, and ultraviolet air disinfection in rooms." *Arch. Environ. Health*, 22: 200-207.

Ross, C., Menezes, J. R. d., Svidzinski, T. I. E., Albino, U., and Andrade, G. (2004). "Studies on fungal and bacterial population of air-conditioned environments." *Brazilian Archives of Biology and Technology*, 47(5), 827-835.

Russo, J.S., and Khalifa, E. (2011). "Computational study of breathing methods for inhalation exposure." *HVAC&R Research*, 17:419-431.

Sandberg, M., and Sjöberg, M. (1983). "The use of moments for assessing air quality in ventilated rooms." *Build.Environ.*, 18(4), 181-197.

Schmidt, M. G., Attaway, H. H., Terzieva, S., Marshall, A., Steed, L. L., Salzberg, D., Hamoodi, H. A., Khan, J. A., Feigley, C. E., and Michels, H. T. (2012).

"Characterization and control of the microbial community affiliated with copper or aluminum heat exchangers of HVAC systems." *Curr.Microbiol.*, 65(2), 141-149.

Sharp, D.G. (1940). "The effects of ultraviolet light on bacteria suspended in air." *J. Bactriol*", 39:535-54.

Shukla, J.B., Singh, V., Misra, A.K.(2011). "Modeling the spread of an infectious disease with bacteria and carriers in the environment". *Nonlinear Analysis: Real World Applications*, 12: 2541–2551.

Singh, P., Mahajan, R. P., Murty, G. E., and Aitkenhead, A. R. (1995). "Relationship of peak flow rate and peak velocity time during voluntary coughing." *Br.J.Anaesth.*, 74(6), 714-716.

Sozer, H., Clark, R. J., and Elnimeiri, M. (2011). "Applying traditional architectural rules for energy efficiency and lateral structural stiffness to an 80 story tower." *Energy*, 36(8), 4761-4768.

Sung, M., and Kato, S. (2010). "Method to evaluate UV dose of upper-room UVGI system using the concept of ventilation efficiency." *Build. Environ.*, 45(7), 1626-1631.

VanOsdell, D., and Foarde, K. (2002) Defining the effectiveness of UV lamps installed in circulating air ductwork. ASHRAE final report. Air-conditioning and refrigeration technology institute 4100N. Arlington, Virginia 22203.

VanSciver, M., Miller, S., and Hertzberg, J. (2011). "Particle image velocimetry of human cough." *Aerosol Science and Technology*, 45(3), 415-422.

Viboud, C., Boëlle, P., Pakdaman, K., Carrat, F., Valleron, A., and Flahault, A. (2004). "Influenza epidemics in the United States, France, and Australia, 1972-1997." *Emerging Infectious Diseases*, 10(1):32-39.

Wainwright, C. E., France, M. W., O'Rourke, P., Anuj, S., Kidd, T. J., Nissen, M. D., Sloots, T. P., Coulter, C., Ristovski, Z., Hargreaves, M., Rose, B. R., Harbour, C., Bell, S. C., and Fennelly, K. P. (2009). "Cough-generated aerosols of *Pseudomonas aeruginosa* and other Gram-negative bacteria from patients with cystic fibrosis." *Thorax*, 64(11), 926-931.

Wang, M., Wolfe, E., Ghosh, D., Bozeman, J., Chen, K. H., Han, T., Zhang, H., and Arens, E. (2014). "*Localized Cooling for Human Comfort*" (No. 2014-01-0686). SAE Technical Paper.

Wan, M., Chao, C., Ng, Y., Sze To, G., and Yu, W. (2007). "Dispersion of expiratory droplets in a general hospital ward with ceiling mixing type mechanical ventilation system." *Aerosol Science and Technology*, 41(3), 244-258.

Wells, W.F. (1934) "On air-borne infection: Study II. Droplets and droplet nuclei.", *American Journal of Epidemiology*, 20 (3), 611-618.

Wells, W. F., Wells, M. W., and WILDER, T. S. (1942). "The environmental control of epidemic contagion I. An epidemiologic study of radiant disinfection of air in day schools." *Am.J.Epidemiol.*, 35(1), 97-121.

Wells, W. F., and Fair, G. M. (1935). "Viability of *B. Coli* Exposed to Ultra-Violet Radiation in Air." *Science*, 82(2125), 280-281.

WHO (1988). *Indoor air quality: biological contaminants*. World Health Organization, European Series, n. 31, Copenhagen, Denmark.

WHO (2004). "WHO guidelines for the global surveillance of severe acute respiratory syndrome (SARS)". Department of Communicable Disease Surveillance and Response, World Health Organization.

Wu, C., Yang, Y., Wong, S., and Lai, A. (2011). "A new mathematical model for irradiance field prediction of upper-room ultraviolet germicidal systems." *J.Hazard.Mater.*, 189(1), 173-185.

Xu, P., Peccia, J., Fabian, P., Martyny, J. W., Fennelly, K. P., Hernandez, M., and Miller, S. L. (2003). "Efficacy of ultraviolet germicidal irradiation of upper-room air in inactivating airborne bacterial spores and mycobacteria in full-scale studies." *Atmos.Environ.*, 37(3), 405-419.

Xu, Z., Shen, F., Li, X., Wu, Y., Chen, Q., Jie, X., and Yao, M. (2012). "Molecular and microscopic analysis of bacteria and viruses in exhaled breath collected using a simple impaction and condensing method." *PloS One*, 7(7), e41137.

Yuill, D., Yuill, G. K., Coward, A. H. (2008). "Measurement and analysis of vitiation of secondary air in air distribution systems (RP-1276)." *HVAC & R Research* 14(3): 345 – 357.

Zhang, Z., and Chen, Q. (2007). "Comparison of the Eulerian and Lagrangian methods for predicting particle transport in enclosed spaces", *Atmospheric Environment*, 41 (25), 1032-1039.

Zhao, B., Zhang, Z., Li, X. and Huang, D. (2004). "Comparison of diffusion characteristics of aerosol particles in different ventilated rooms by numerical method", *ASHRAE Transactions*, 110: 88-95, Part 1.

Zhu, S., Srebric J., Rudnick S.N., Vincent R.L., Nardell E.A. (2013). "Numerical investigation of upper-room UVGI disinfection efficacy in an environmental chamber with a ceiling fan." *Photochemistry and Photobiology*, 89: 782–791.